ROYAL BELGIAN INSTITUTE FOR NATURAL SCIENCES
OPERATIONAL DIRECTORATE NATURAL ENVIRONMENT

Section Ecosystem Data Analysis and Modelling
Suspended Matter and Sea Bottom Modelling and Monitoring Group (SUMO)

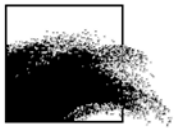

Analysis of climate changes in the time series of wind speed, significant wave height and storm surges at the Belgian coast

Dries Van den Eynde, Stéphanie Ponsar, Patrick Luyten and José Ozer

CREST/X/DVDE/201906/EN/TR03

Prepared for the CREST project

RBINS-OD Nature
Vautier street 29
B–1000 Brussels
Belgium

Table of Contents

I. Introduction

In the framework of the CREST project, the influence of the climate changes on hydrodynamic parameters on the Belgian Continental Shelf (BCP) is investigated. In this report, the influence on the wind speed at Westhinder, the significant wave height at Bol van Heist and the storm surges at Ostend are assessed.

The atmospheric conditions (atmospheric pressure and wind speed) are taken from seven regional climate models, which were prepared in the framework of the CORDEX.be project or were downloaded from the CORDEX data base. For the current climate, a historical run was performed covering a 30 years period (1976-2005). To investigate the effect of the climate change, simulations were performed for the RCP 8.5 scenario (Representative Concentration Pathways) of the International Panel for Climate Changes (IPCC). The RCP 8.5 scenario is the 'worst-case scenario' for future emissions, ending with a radiative forcing of 8.5 W/m² by 2100. This is the scenario that receives the most attention and was mostly used in the framework of the CORDEX.be project. A similar period of 30 years was simulated, from 2070 to 2099. To evaluate the influence of the forcing model, the actual weather was also modelled by three models, forced with the data from the reanalysis of ERA-INTERIM model from the ECMWF (https://www.ecmwf.int/en/research/climate-reanalysis/era-interim) for the period 1980-2010.

The significant wave heights were modelled using the WAM model. The WAM model is a third-generation wave model, developed by the WAMDI Group (1988) and described by Günther *et al.* (1992). The WAM model includes 'state-of-the-art' formulations for the description of the physical processes involved in the wave evolution. In comparison with the 2nd generation model, the wave spectrum has no restriction and the wind sea and the swell spectrum are not treated separately. At the Operational Directorate Natural Environment, the model is run on three coupled model grids. A Coarse model grid comprises the entire North Sea, the Fine grid covers the central North Sea and the Local grid is used for the Southern Bight. The local grid has a resolution of 0.033° in latitude and 0.022° in longitude. The WAM model was validated using UKMO meteorological forecasts (e.g., Van den Eynde, 2013).

For the storm surges, the hydrodynamic COHERENS model is used (Luyten *et al.*, 2016), calculating the currents and the water elevations on the entire North West European Continental Shelf with a resolution of 4 km by 4 km. A first validation of the model was executed by Ozer *et al.*, 2017, using the ALARO forecasts. The model proved to give satisfactory results.

In the first section the meteorological forecasts are discussed and compared with each other to have some insight in the accuracy of the simulated climate. The following section discusses the methodology to derive from the simulated time series the distribution of the extreme events and the values for certain return periods. The quantile mapping method is discussed as well, which is used to correct the biases of the model results. In the next three sections, the results for the wind speed, the significant wave height and the storm surges are discussed. A last section comprises some discussion of the results.

2. Meteorological predictions

2.1. *Data files*

In the current framework, eight different meteorological forcings, including wind speed and atmospheric pressure, are being used, which are summarized in Table 1.

The first two meteorological forcings were prepared in the framework of the Brain.be project CORDEX.be (Termonia *et al.*, 2018; Giot *et al.*, 2018). The ALARO model has been run by the Belgian Royal Meteorological Institute (RMI), while the COSMO simulations were performed by the Catholic University of Leuven (Vanden Broucke *et al.*, 2018). A comparison between the ALARO and the COSMO models is given in Helsen *et al.*, 2019. While the ALARO results have a time resolution of 3h, the COSMO results are given at a higher temporal resolution of 1h. Both datasets have a spatial resolution of 12.5 km x 12.5 km.

Table 1: Overview of the meteorological conditions

Model	Source	EVAL	HIST	RCP8.5	Time resolution	Grid
ALARO	CORDEX.be	X	X	X	3h	ALARO
COSMO	CORDEX.be	X	X	X	1h	COSMO
CNRM	CORDEX		X	X	6h	EUR11
ECMWF	CORDEX	X			6h	EUR11
ICHEC	CORDEX		X	X	6h	EUR11
IPSL	CORDEX		X	X	6h	EUR11
MOHC	CORDEX		X	X	6h	EUR11
MPI	CORDEX		X	X	6h	EUR11

The ALARO grid is based on a Lambert Conformal grid (longitude of the central meridian: 9.9°, the latitude of the projection origin: 49° and the standard parallel: 49°). The positions of the grid points are presented in Figure 1. The total grid has 485 x 485 grid points. The COSMO grid is a rotated North Pole grid (latitude of North Pole: 39.25°, longitude of North Pole: -162.0°). This grid has a total of 450 x 438 grid points. These grids are presented in Figure 2.

The six other meteorological forecasts were downloaded from the CORDEX data base (e.g., https://esgf-index1.ceda.ac.uk/projects/esgf-ceda/): data from the Centre National de Recherches Météorologiques, France (CNRM), European Centre for Medium Range Weather Forecast, U.K. (ECMWF), Irish Centre for High-End Computing, Ireland (ICHEC), Institut Pierre-Simon Laplace, France (IPSL), Met Office Hadley Centre, U.K. (MOHC) and Max Planck Institute for Meteorology, Germany (MPI), were used.

The results of regional climate models with a high spatial resolution (12.5 km x 12.5 km) and a temporal resolution of at least 6h were selected. Six different model results could be found, see Table 1. All these models use the EUR11 model grid, which has the same rotated North Pole as the COSMO grid, but covers a slightly smaller area (412 x 412 grid points). The positions are presented in Figure 3.

For the current climate, a historical run (HIST) was performed by seven models (see Table 1). It covers a period of 30 years, from 1976 to 2005. To investigate the effect of the climate change, simulations were performed by the same models for the RCP 8.5 scenario of the International Panel for Climate Changes (IPCC). This is the scenario that receives the most attention and was mostly used in the framework of the CORDEX.be project. A period of 30 years was simulated, from 2070 to 2099.

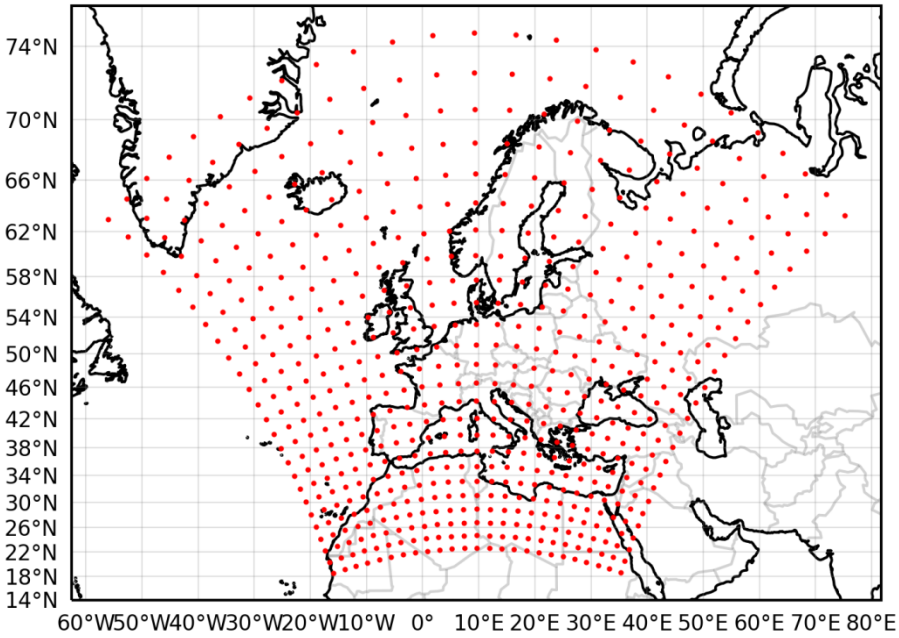

Figure 1: Model grid of the ALARO meteorological predictions. One point is shown for every 20 points in both directions.

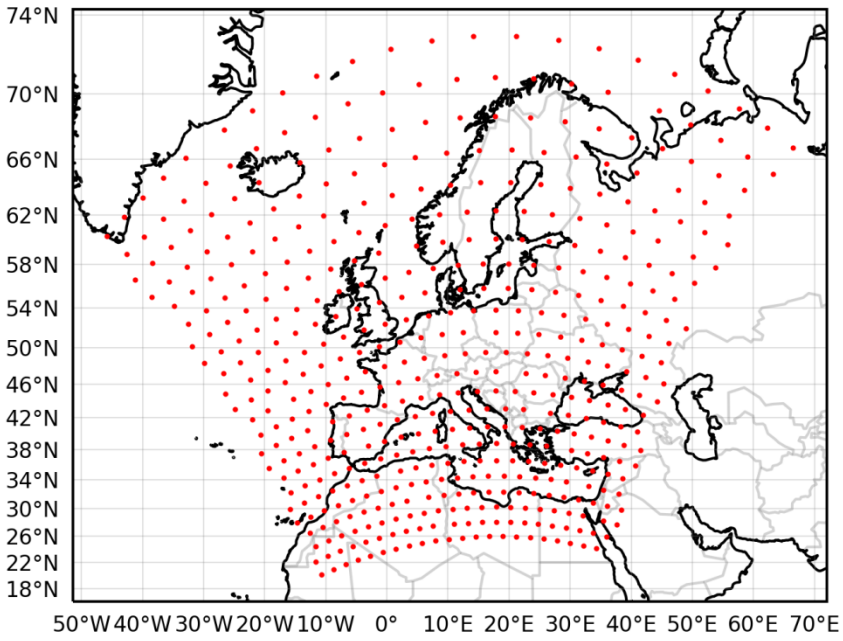

Figure 2: Model grid of the COSMO meteorological predictions. One point is shown for every 20 points in both directions.

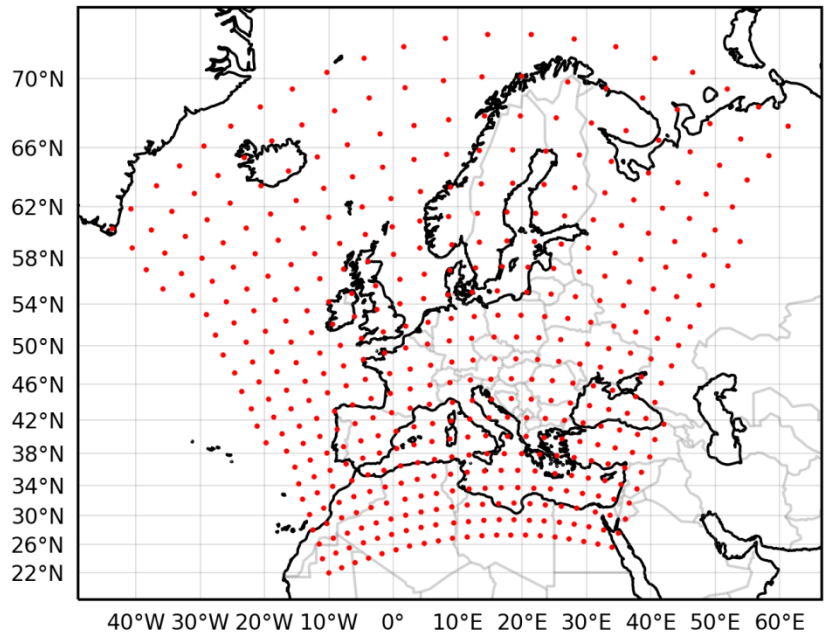

Figure 3: Model grid of the EURI I meteorological predictions. One point is shown for every 20 points in both directions.

For the historical runs, all regional climate models were driven by the results of a global climate model. To evaluate the influence of this forcing, two of these regional climate models, *i.e.,* ALARO and COSMO, were run for a 30 years period (1980-2010) but now forced with the data from the reanalysis of ERA-INTERIM model from the ECMWF (https://www.ecmwf.int/en/research/climate-reanalysis/era-interim). These simulations are referred to as the evaluation runs (EVAL). The results of the ECMWF regional model were also available for the same period. While the historical simulations should represent the current climate, but not really the weather over the period 1976-2005, the evaluation simulations should well represent the weather over the period 1980-2010 and could be used to 'validate' the regional climate models. Both types of simulations however should represent the current climate, i.e., representing the same trends.

It is important to notice that meteorological predictions for other RCP scenarios are available and that for the RCP 8.5 scenario, other periods are available (2000-2069). However, this first study will be focused on the changes between the historical (current) climate and the RCP 8.5 scenario by the end of the century, for which the largest changes can be expected.

2.2. *First analysis of the meteorological predictions*

2.2.1. Measurements at Westhinder

Measurements at Westhinder were obtained from the Meetnet Vlaamse Banken (Vlaamse Gemeenschap, Agentschap Maritieme Dienstverlening en Kust) for the period March 1994 to September 2015, a period of more than 20 years. However, some of the measured data were taken with different time resolutions. To compare them with the data from the different meteorological forecasts for the evaluation runs, the measurements were averaged over a time resolution of 1h (to compare with COSMO), 3h (compare with ALARO) or 6h (compare with ECMWF). Remark that the time averaging procedure clearly has some influence on the actual values, especially on the maximum values (Figure 4).

In Figure 5, Figure 6 and Figure 7 respectively the bias, the Root-Mean-Square-Error (RMSE) and the correlation coefficient are presented for the different years. In addition to the meteorological predictions of the ALARO, COSMO and ECMWF evaluation runs, also the meteorological data from the UKMO are included in the validation. These are the data that are twice a day obtained by the RBINS-OD Nature to be used for the operational forecasts of the surges and waves. Note that these data have a time resolution equal to 6 hours.

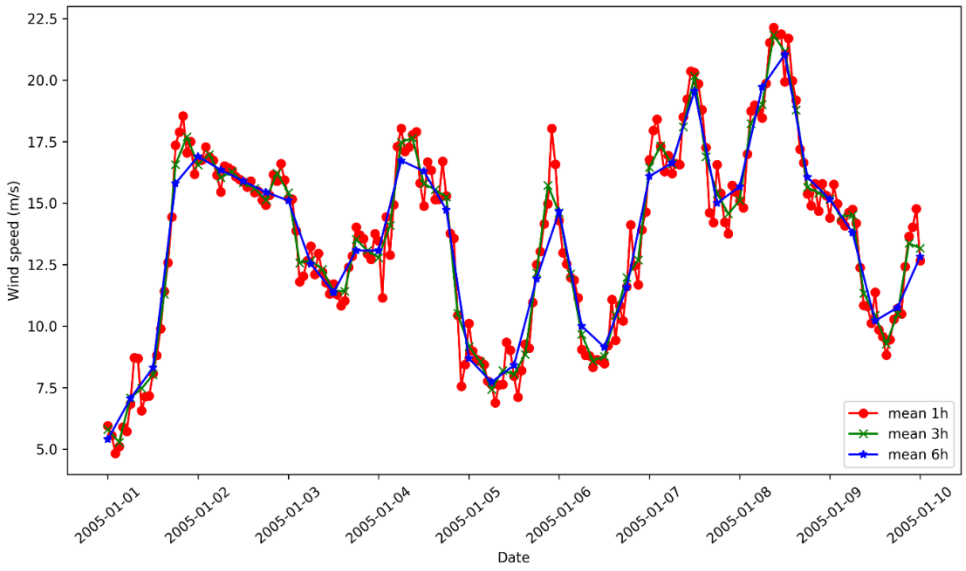

Figure 4: Wind speed measurements 1/1/2005-10/1/2005, and influence of period over which the data are averaged.

Figure 5 shows that all models seem to under predict the yearly mean wind speed with a negative bias between -0.5 m/s and -2.5 m/s, while the overall mean wind speed of the measurements is 8.7 m/s. Surprisingly the bias is the largest for the UKMO meteorological predictions. The lowest bias is found for the ECMWF meteorological predictions, as could be expected, while the ALARO and the COSMO meteorological forecasts are similar. The biases for the seven historical runs are included in the figure as well. These historical runs represent the same climate, but do not simulate the actual weather. The biases of these different runs are in the same order of magnitude, between -3 m/s and 0 m/s.

In Figure 6, the RMSE is shown for the evaluation runs and the historical runs. Here it is clear that the historical runs do not represent the actual weather. The RMSE is higher for the different historical runs than for the evaluation runs. However, also for the evaluation runs, the RMSE is relatively high, with RMSE varying between 2.5 and 4 m/s. The best results are here obtained by the UKMO forecasts, while the ALARO forecasts gives the largest RMSE. In this case the COSMO evaluation run is better than the ECMWF evaluation run. In Annex 1, also the systematic and non-systematic RMSE are presented.

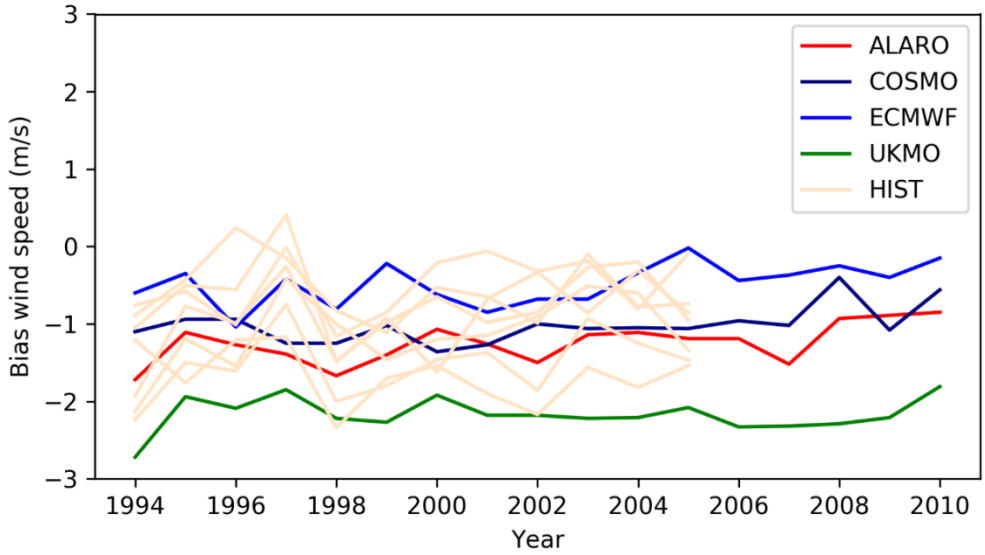

Figure 5: Bias between the evaluation runs results for the ALARO, COSMO, ECMWF and UKMO data sets and the measurements at Westhinder.

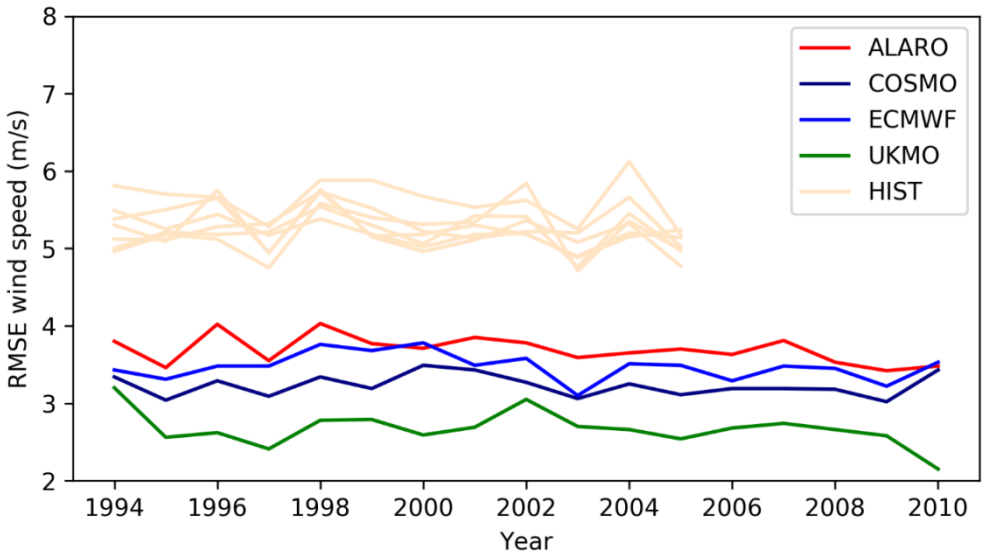

Figure 6: RMSE between the evaluation runs results for the ALARO, COSMO, ECMWF and UKMO data sets and the measurements at Westhinder.

Finally, in Figure 7, the correlation coefficients are presented between the evaluation runs and the measurements. Although the historical runs (should) represent the actual climate, the predictions do not represent the actual weather. The correlation is between -0.05 and 0.2 for all runs. The UKMO meteorological forecasts clearly give the best results. The correlation for the COSMO meteorological predictions is better than the results for the ALARO and the ECMWF meteorological predictions, which have a correlation coefficient around 0.6.

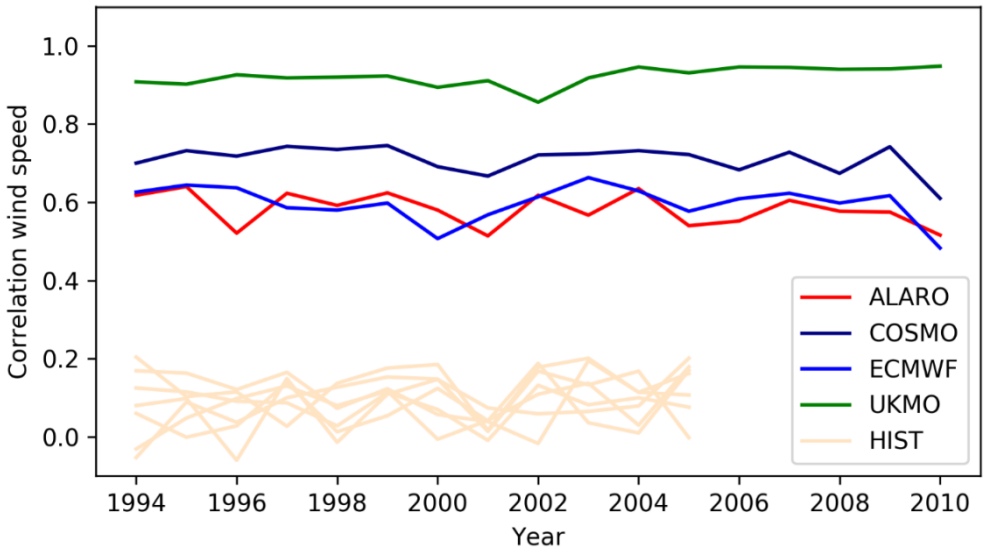

Figure 7: Correlation coefficient between the evaluation runs results for the ALARO, COSMO, ECMWF and UKMO data sets and the measurements at Westhinder.

To summarize, one can conclude that the results of the UKMO meteorological forecasts are clearly better than the results from the regional climate models. This is probably due to the data assimilation which is used in the operational forecasts. The relatively poor results comparing the evaluation run results with the measurements at Westhinder should be taken into account when analyzing the results.

2.3. *Comparison of mean wind speeds*

Before analysing the results of the extreme wind speeds, the differences between the mean wind speeds over the entire WAM model grid (covering the North Sea) are analysed. Both the differences between the evaluation run and the historical run and the difference between the historical run and the climate run (scenario RCP 8.5) are analysed.

Although the evaluation run and the historical run should represent the same current climate, some differences were clearly observed, both for the ALARO and for the COSMO predictions. In Figure 8, the mean wind speed over the North Sea for the ALARO evaluation run and the historical run are shown, for an equal period of 30 years. The differences between them are shown in Figure 9. In the northern North Sea, higher wind speeds are, on average, encountered for the evaluation run. This could have some implication on the storm surges and the waves, also in the southern North Sea. In the southern North Sea itself, the differences are less important. For the COSMO meteorological predictions, the differences between the evaluation run and the historical run are less important (see Figure 9).

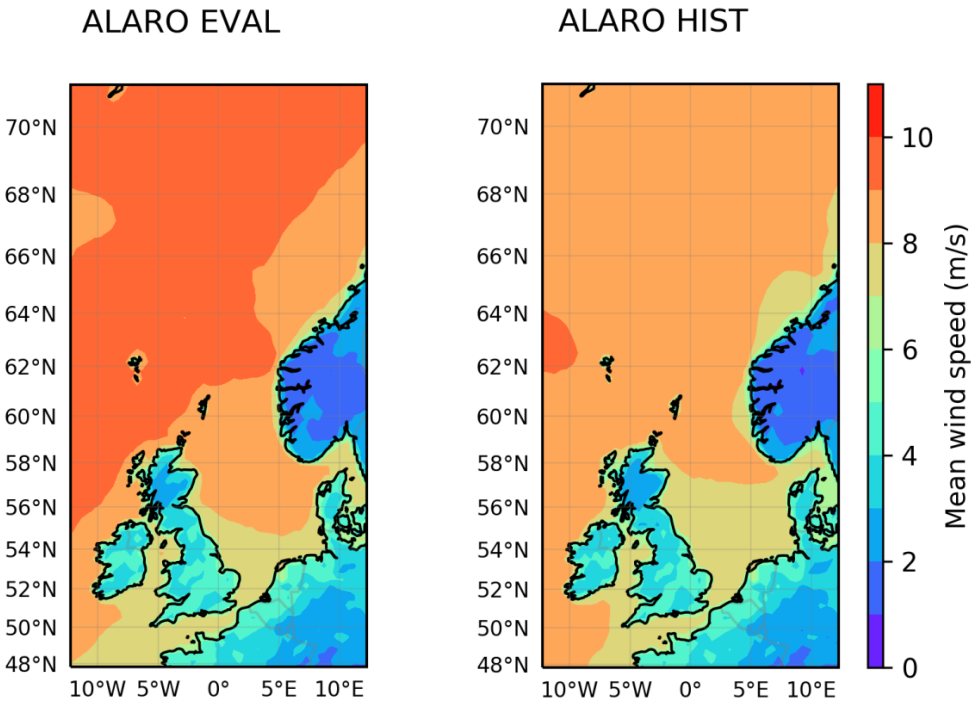

Figure 8: Mean wind speed map for the ALARO evaluation run and historical run.

For the climate studies, performed here, the differences between the historical runs and the climate runs, scenario RCP 8.5, are more important. For the seven regional climate models, these differences are shown in Figure 10 and Figure 11. The differences between the average wind speed of the historical runs and the RCP 8.5 runs are relatively small. There are some differences to be remarked however. While in the COSMO and the ICHEC results, a small decrease in mean wind speed can be observed in the northern North Sea, an increase in mean wind speed is observed for the MOHC results. For completeness, all maps of the mean wind speed for the different models, together with the maps of the standard deviations of the wind speeds at the grid locations are presented in Annex 2. One can notice that there are important differences between the different model results.

Remark that a comparison of future evolution of wind fields is also presented in Devis *et al.* (2018).

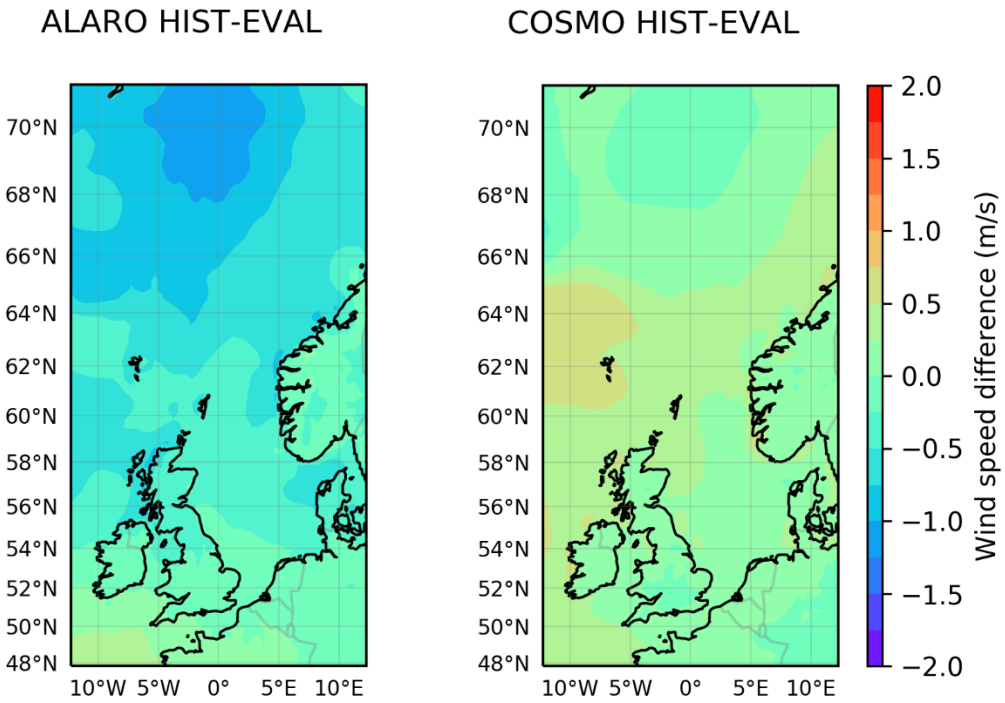

Figure 9: Difference in mean wind speed map for the ALARO and the COSMO historical and evaluation run.

This is also illustrated in Figure 12 were for three stations the mean wind speed over the entire period is given for the different regional climate models and for the different simulations. Beside results at the station Westhinder, in front of the Belgian coast, also results in a station at the North of the domain (0°, 70°N) and in the West of the domain (10°W, 66°N) are presented (see Figure 39 for the positions). One can see that for the station Westhinder, the differences between the mean wind speed in the historical runs and the RCP 8.5 runs are small, except for the ICHEC model where the RCP 8.5 mean wind speeds are smaller than those of the historical run. For the northern station, the differences are small as well. Only for the western station, larger differences are obtained with however sometimes contradicting results: while the mean wind speed is larger in the RCP 8.5 simulation for the COSMO and the ICHEC models, the RCP 8.5 simulation obtains smaller mean wind speeds for the MOHC simulations.

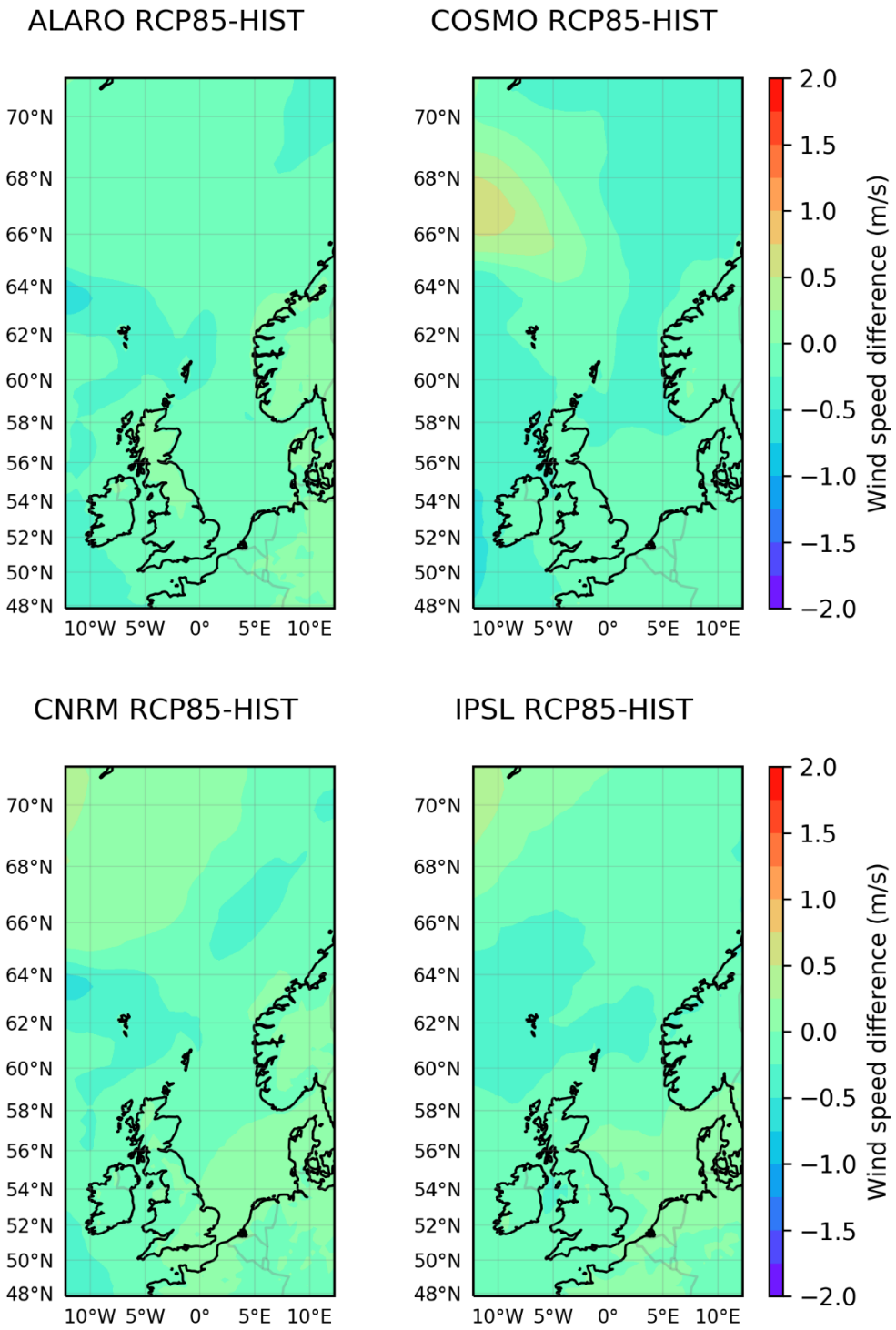

Figure 10: Difference in mean wind speed map for the ALARO, COSMO, CNRM and ICHEC historical run and climate RCP 8.5 run

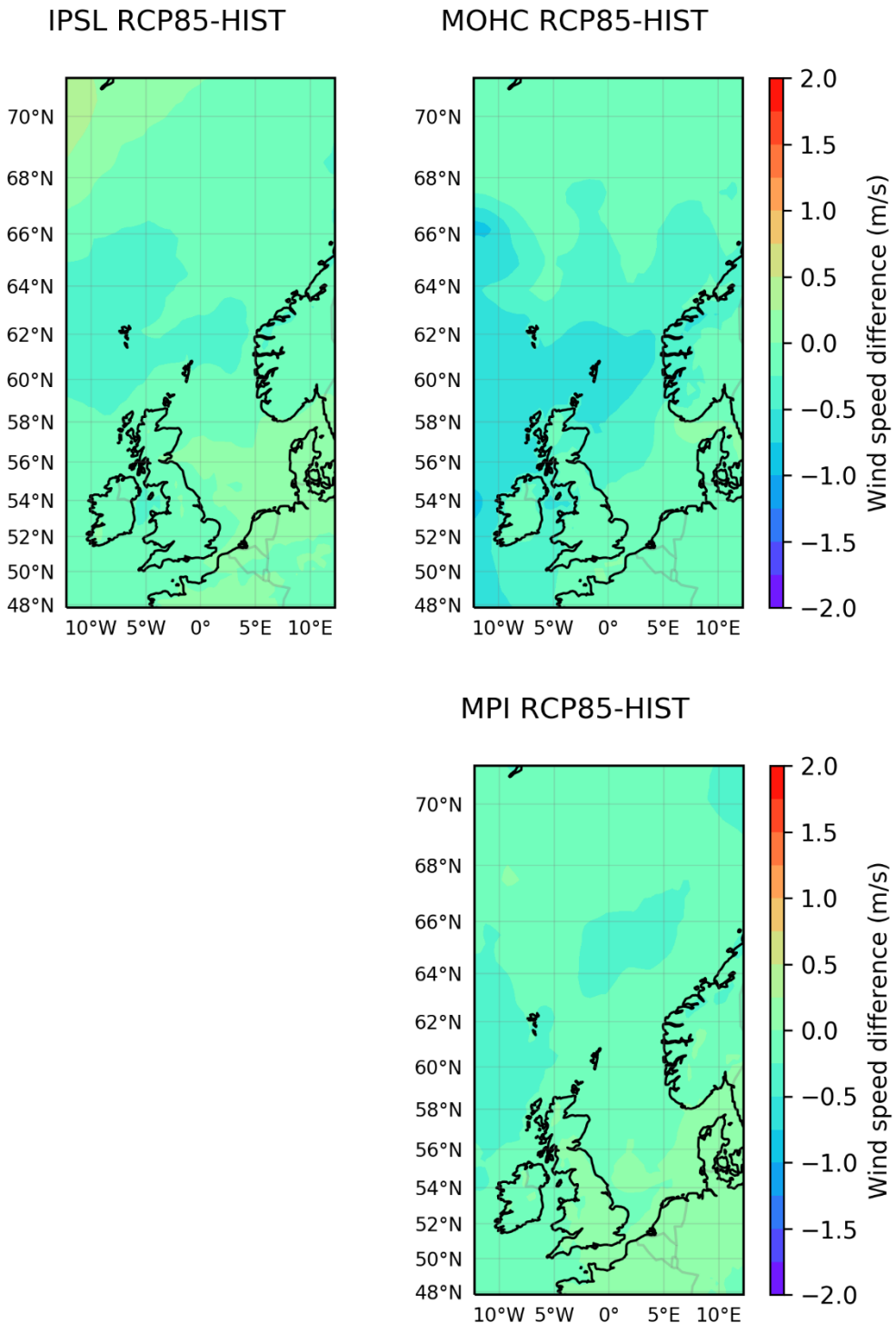

Figure 11: Difference in mean wind speed map for the IPSL, MOHC and MPI historical run and climate RCP 8.5 run.

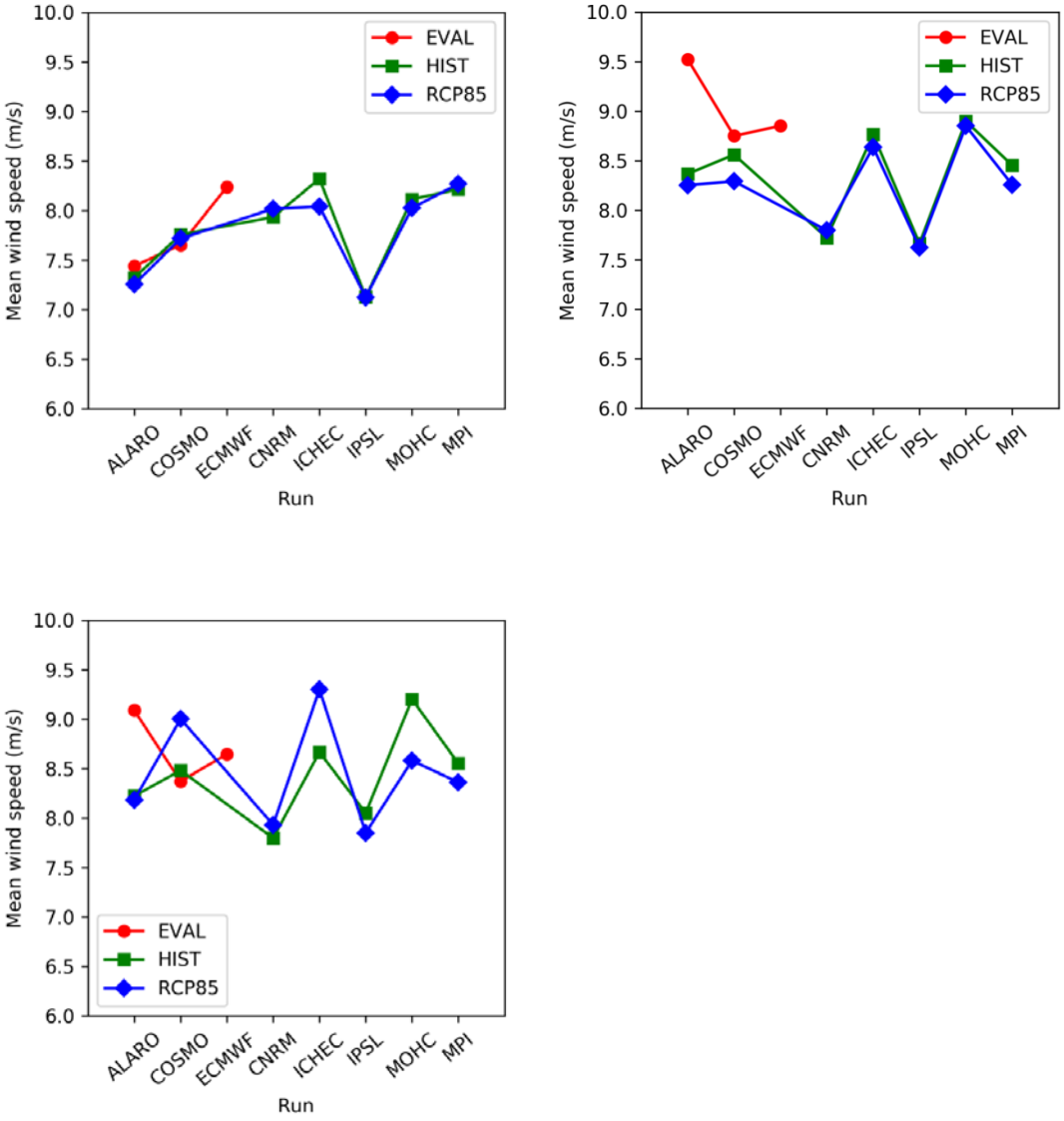

Figure 12: Mean wind speed at Westhinder (left upper), station North (right upper) and station West (left below) for the different models and different runs.

2.3.1. Comparison of high wind speeds

Because the high waves are mainly produced by high wind speeds, also the differences between the occurrences of high wind speeds over the North Sea are analysed. The differences between the evaluation runs and the historical runs and those between the historical runs and the climate runs (scenario RCP 8.5) are analysed separately.

In Figure 13, the percentage of time that the wind speed is over 20 m/s is shown for the ALARO evaluation run and the historical run. One can observe that the evaluations run shows more frequent high wind speeds especially in the northern North Sea. The differences are shown in Figure 14. The differences

between the percentage of wind speeds higher than 20 m/s for the evaluation run and the historical run of the COSMO meteorological predictions are shown as well. They are less important.

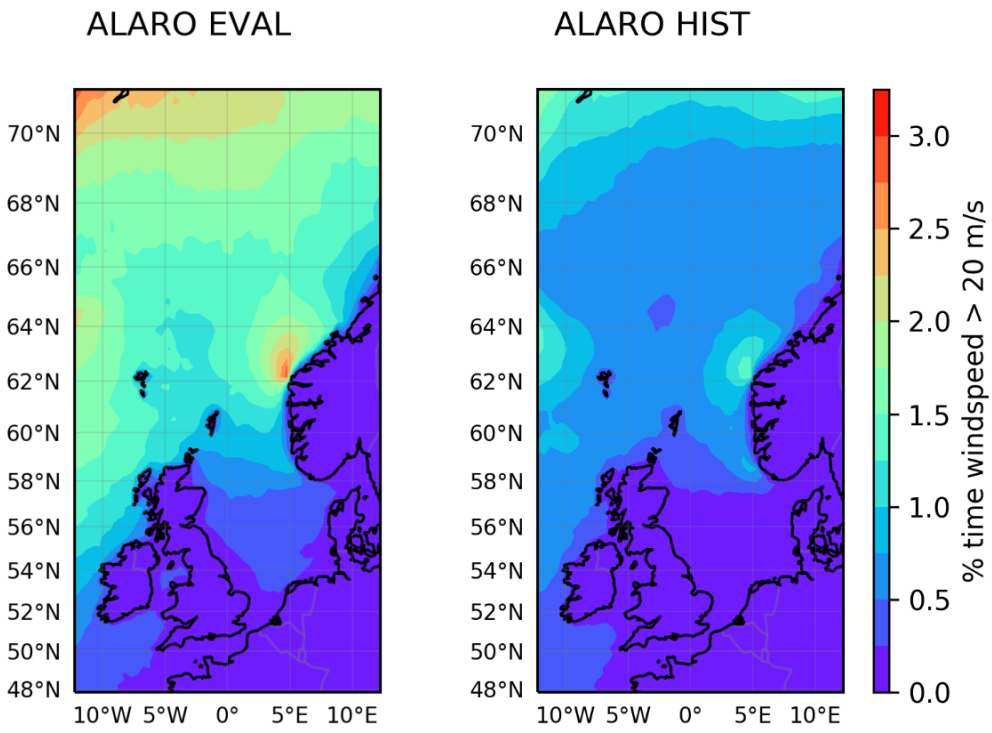

Figure 13: Percentage of high wind speeds map for the ALARO evaluation run and historical run.

Remark however that differences are might be low, but that the percentage itself is low as well, so that the relative change in percentage of high winds (above 20 m/s) can be high. This is also shown in Figure 14. Remark that the white zones, mostly over land, are zones where the relative difference is higher than 100%.

For the climate studies, performed here, the differences between the historical runs and the climate runs, scenario RCP 8.5, are more important. In Figure 15, the results are shown for the ALARO, COSMO, ICHEC and MOHC predictions. For the ALARO model, the results are relatively small, as for the IPSL and the MPI models (not shown). For the ICHEC model, a small region is found where there is an increase in the percentage of high wind speeds. For the COSMO and the MOHC models however, there is a clear decrease in high wind speeds in the RCP 8.5 results, certainly in the western part of the grid, north-west of Ireland.

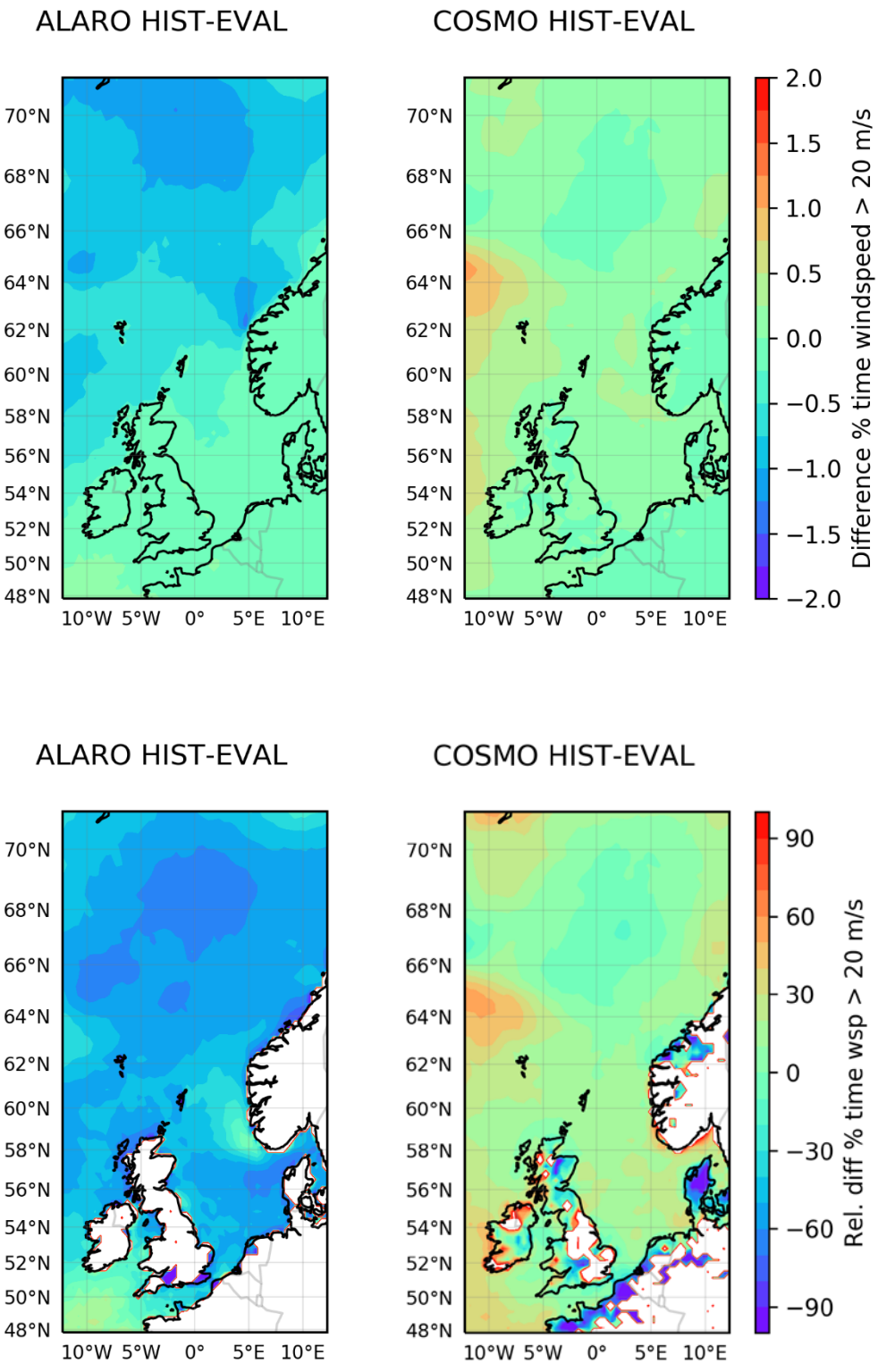

Figure 14: Difference in percentage of high wind speeds map for the ALARO and the COSMO evaluation and historical run. Upper plots: absolute difference; lower plots: relative difference (w.r.t. evaluation).

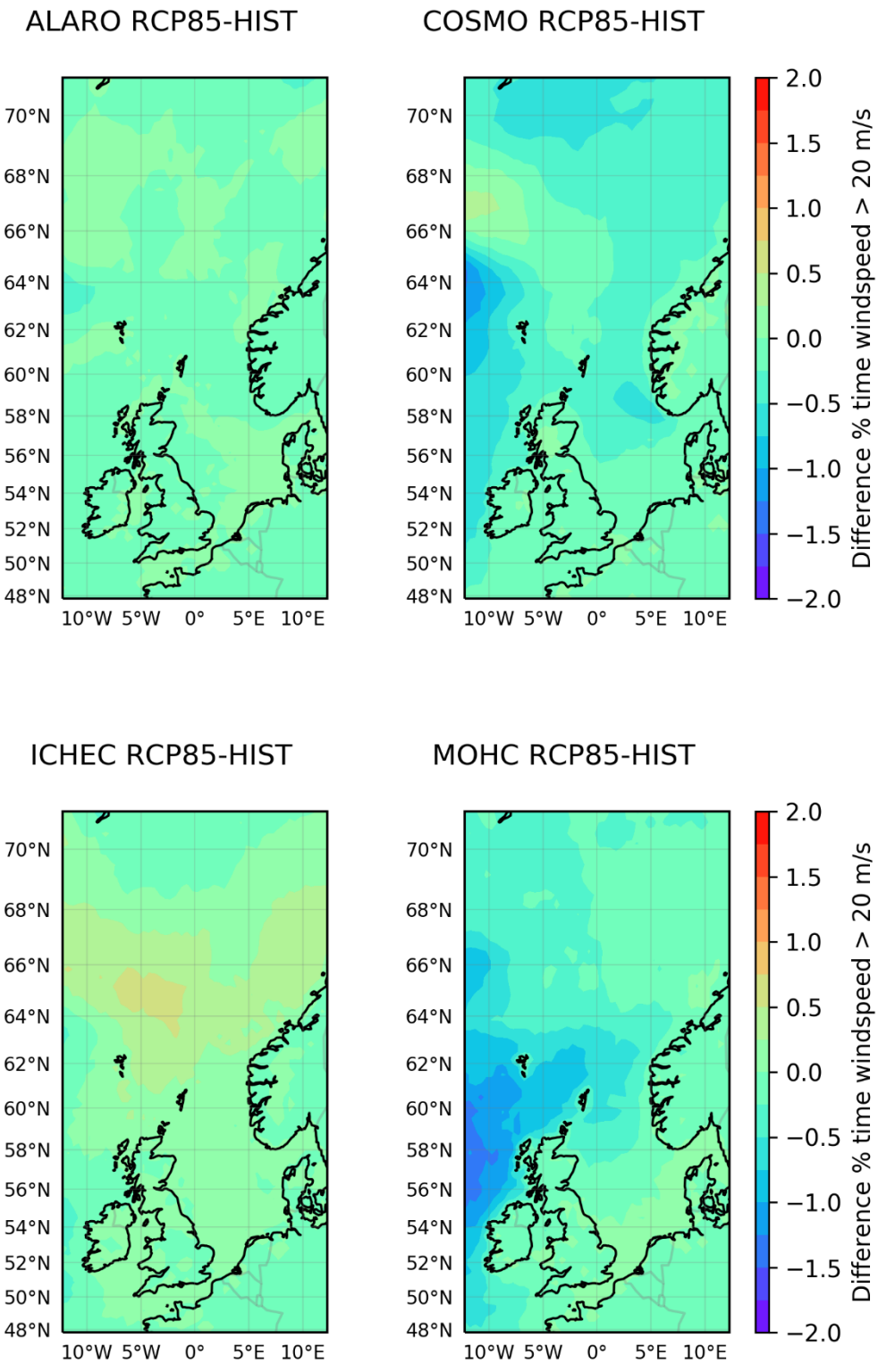

Figure 15: Difference in percentage of high winds speed map for the ALARO, COSMO, ICHEC and MOHC historical run and climate RCP 8.5 run.

3. Methodology

3.1. *Extreme events and return periods*

The method that is used to evaluate the time series and to extrapolate the data to extreme values with a certain return period is based on the work of Kamphuis (2010).

To evaluate a time series, first the "extreme events" in the time series are selected. A certain threshold or critical value is defined and for each period for which the threshold is passed, the maximum value during that period is used to characterise the extreme event (see Figure 16). Remark that Kamphuis (2010) showed that the exact value of the threshold is not critical. As an example, the number of storms with a significant wave height higher than 1.8 m at Bol van Heist is shown for the results of the ALARO evaluation run in Figure 17. A total number of 827 storms were encountered during the 30 years period. Amongst these, 162 had a maximum significant wave height between 1.80 m and 1.92 m, while only one storm had a maximum significant wave height between 4.56 m and 4.68 m.

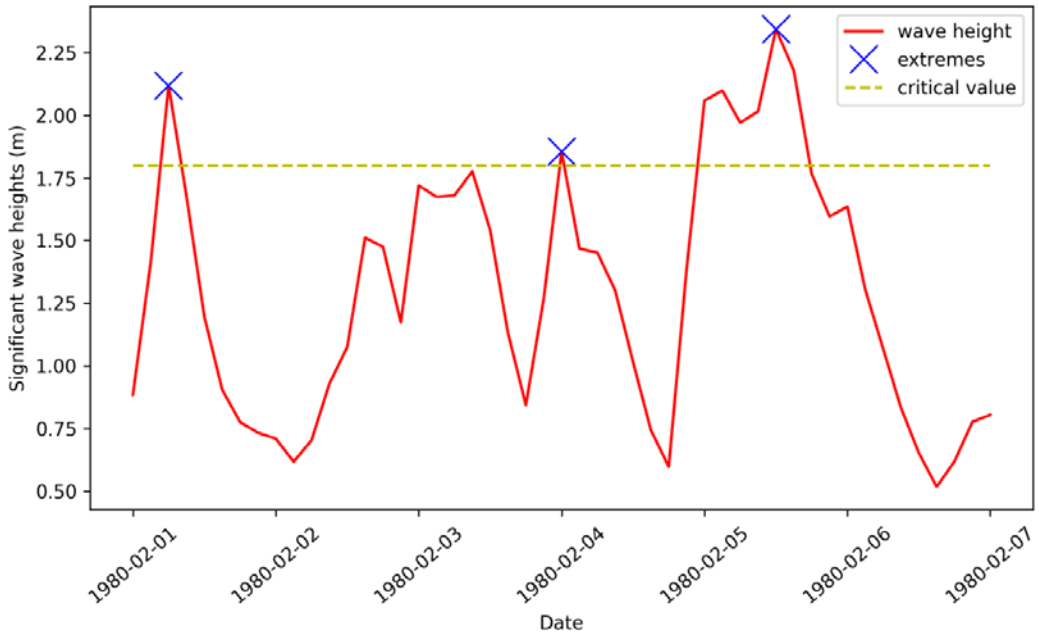

Figure 16: Definition of extreme events

From this list of extreme events, a cumulative probability function is then made as a function of a certain value. For a certain value, the probability is calculated that, when an extreme event happens, the maximum reached during this event, is lower than this value (see Figure 18). This cumulative distribution is then changed in a cumulative probability function, by dividing by the total number of storms. By using (1 – Probability), the density probability function is obtained that gives the probability that during a storm, a certain significant wave height is reached (see

Figure 19).

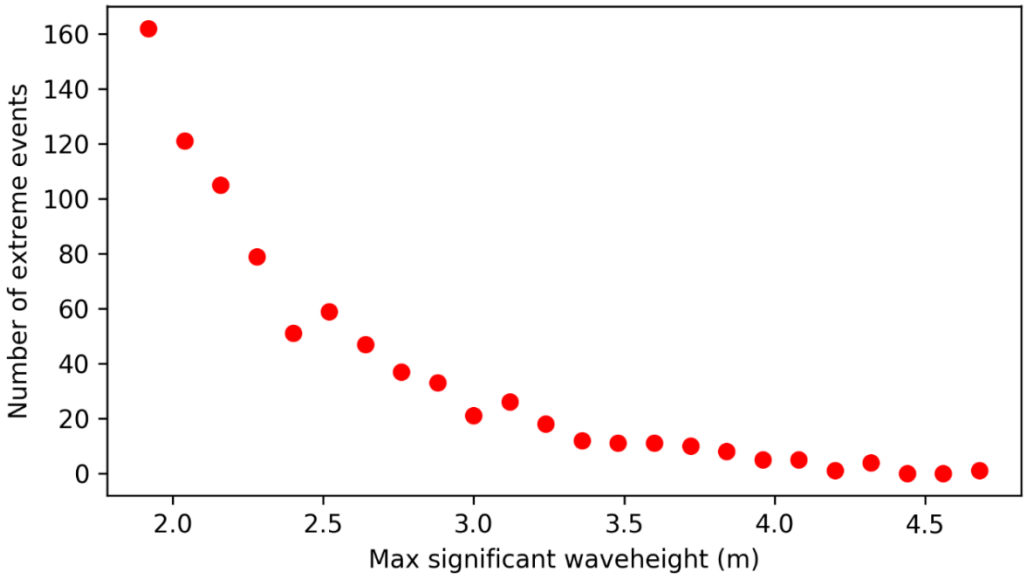

Figure 17: Number of storms during the period 1980-2009 with a maximum significant wave height, for the results of the ALARO evaluation run.

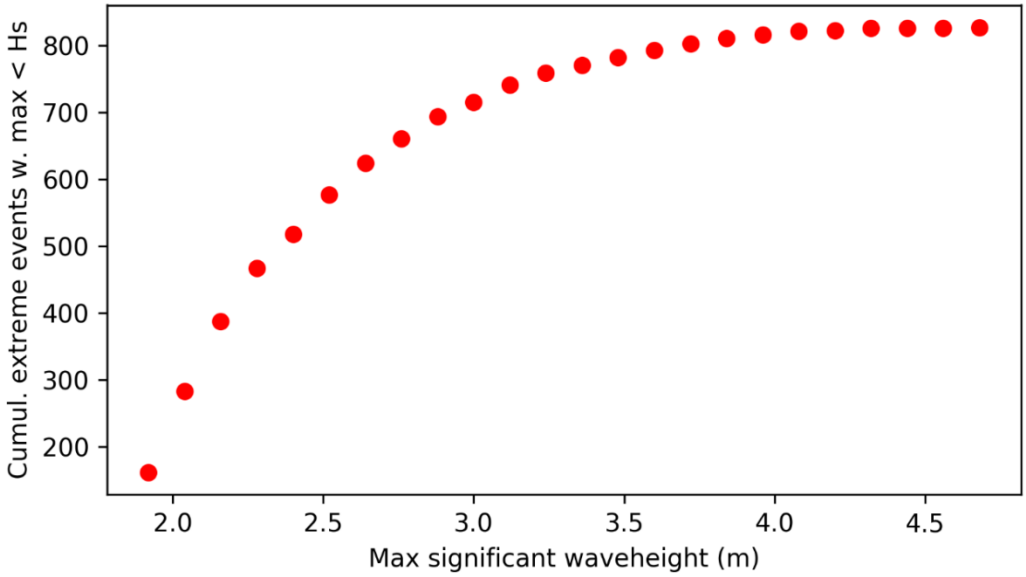

Figure 18: Cumulative number of storms during the period 1980-2009 with a maximum significant wave height lower than a specified value, for the results of the ALARO evaluation run.

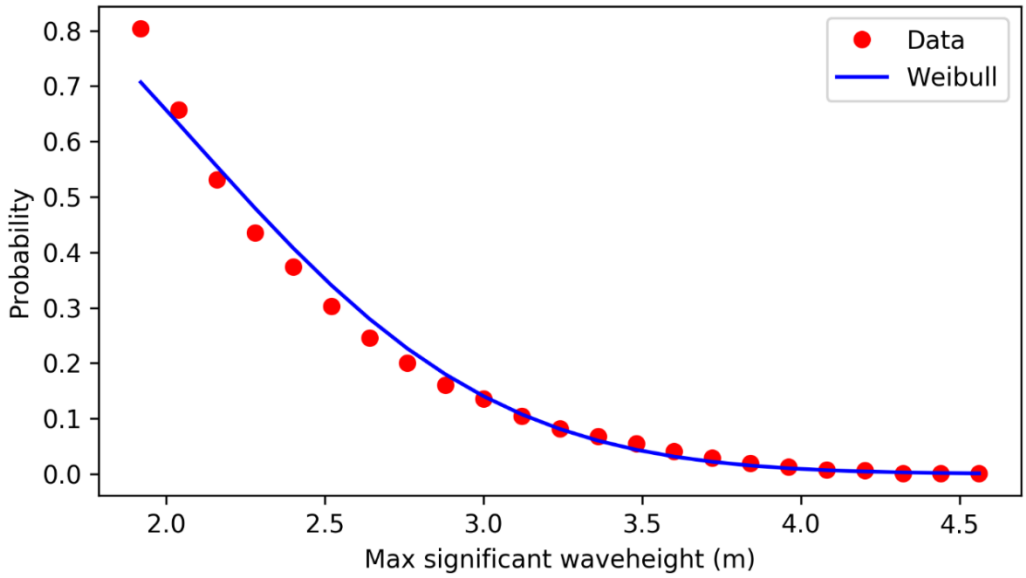

Figure 19: Probability that during a storm a certain significant wave height is reached during the period 1980-2009 in the results of the ALARO evaluation run.

This cumulative probability function can be parametrised by different (extreme value) functions. In this study, some tests were executed with the Normal distribution, Log-Normal distribution, the Gumbel distribution and the Weibull distribution, as proposed by Kamphuis (2010). Remark that in the Weibull distribution, an additional parameter α is used. Remark that in recent literature, also the Generalized Extreme Value (GEV) distribution is regularly used.

Tests showed that the Weibull distribution gave the best results and is therefore used in this study. To fit the Weibull distribution, the equations were linearized first, so that a least square regression analysis could be used to find the fitting parameters. More information can be found in Kamphuis (2010). In Figure 19 the fitted Weibull distributions is also shown.

The advantage of the fitted Weibull distribution is that using this distribution, also extrapolation to longer periods can be executed. This can for instance be used to calculate the maximum wave height that can be expected for a certain return period. Remark that the number of storms during a year needs to be taken into account.

3.2. *Bias correction by quantile mapping*

From the previous sections, it was already clear that the meteorological predictions from the different regional climate models do not always give the same results. Furthermore, there are clearly some differences between the evaluation runs and the historical runs for the ALARO and the COSMO models, and between the different historical runs from the other regional climate models. However, all these meteorological predictions should perfectly represent the current climate. The climate simulations should be compared, in principle, with the current climate, to be able to evaluate the variations caused by climate changes. When the climate run

results would be used, without correction, a large part of the variability of the results would not only be due to the effect of climate change, but also to the fact that the current climate is not perfectly well represented. Therefore, some bias correction is executed first. Here it is assumed that the corrections required to fit the results of the historical simulations with the current climate, can also be used to correct the climate simulations. In this case, the current climate is represented by the observations.

In literature, different possibilities for bias correction can be found. Recent studies, mainly in hydrology, compared different possibilities and showed that the best results could be obtained with the quantile mapping method. This simple method is used in this study as well.

In this method (see Fang *et al.*, 2015) the corrected probability P_{corr} is calculated from the probability P_{ori} using the original cumulative distribution function (CDF_{ori}) and the inverse of the observed (correct) cumulative distribution function CDF_{obs}:

$$P_{corr} = CDF_{obs}^{-1}(CDF_{ori}(P_{ori}))$$

For each extreme value, the probability in the original CDF is therefore corrected. In the case of the results of the historical run, the correction is such that the corrected value is the same as the observed probability. The same correction is also used then for the results of the RCP 8.5 simulations. From the corrected cumulative distribution function, the extreme values for a certain return period can be calculated.

4. Analysis of wind speed

4.1. *Measurements at Westhinder*

The analysis of the changes in extreme wind speeds due to climate changes on the Belgian coast is executed for the station Westhinder. Observations were obtained from the Meetnet Vlaamse Banken (Vlaamse Gemeenschap, Agentschap Maritieme Dienstverlening en Kust) with a time step of 10 minutes. The time series that was available covered a period from 30/3/1994 to 29/9/2015, a period of more than 20 years, without too many data gaps. To be compatible with the time resolution of the meteorological predictions, the data were averaged over periods of 1 h, 3 h and 6h.

Extreme wind events are defined here when the wind speed at Westhinder is larger than 15 m/s, stored in bins of 0.4 m/s.

As mentioned above, the averaging of course influences the number of extreme events. While there are 100 extreme events, with wind speeds higher than 15 m/s, when the time series are averaged over 1 h, there are only 56.9 or 41.3 extreme events, when averaged over 3 h or 6 h respectively.

In Figure 20, the probabilities and the Weibull distributions are shown for the measurements, averaged over 1h, at Westhinder. The Weibull distributions for the measurements, averaged over 3 h or over 6 h, will differ a little bit. Since the results of the historical runs (and the climate runs) will be corrected, this is not essential to evaluate the influence of the climate change on the results.

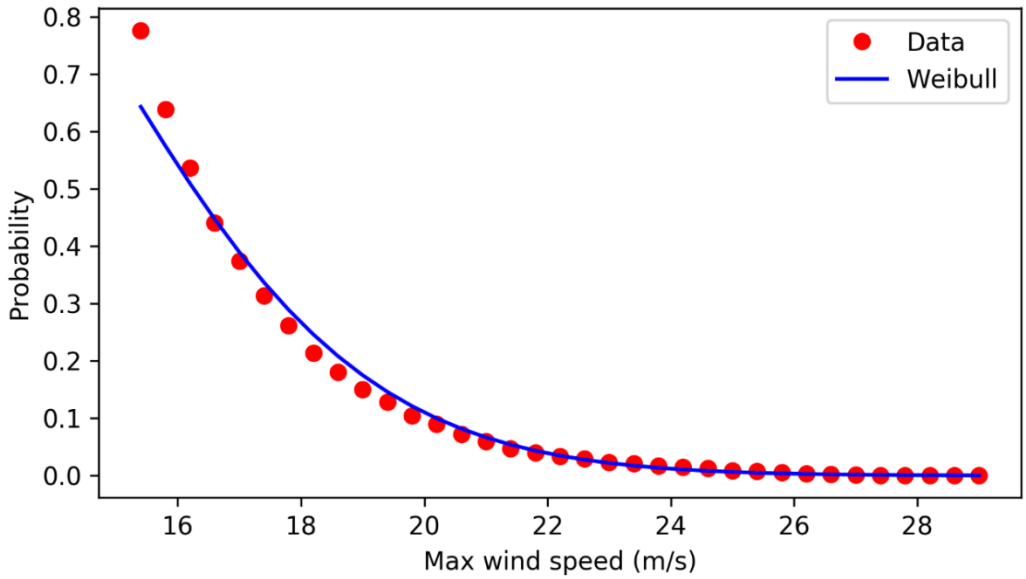

Figure 20: Probability that during a extreme event a certain wind speed is reached in the measurements at Westhinder.

4.2. *Analysis of the model results*

In Table 3 the number of "extreme" events per year (wind speed higher than

15 m/s) is given together with the maximum wind speed observed during the period. The number of extreme events varies between 16.9 events for the IPSL model to 61.4 events for the COSMO model. The number of extreme events is higher for the COSMO model is partly due to the fact that the time resolution of the COSMO model is 1 h, while the time resolution for the other models is 3 h (ALARO) or 6 h (other models). This is also seen in the measurements where there are more extreme events per year, when the measurements are averaged over 1 h, than when the measurements are averaged over 3 h or 6 h. Remark however that accounting for the time resolution the measurements still show more extreme events than the model results. When comparing the number of extreme events in the historical simulation with the climate simulations, the differences are small, with for four models a decrease in the number of extreme events, while this number increases for three models. It is therefore not easy to draw clear conclusions from this. The number of extreme events per year is also shown in Figure 21.

When comparing the maximum wind speeds found over the period, it is remarkable that five models see an increase in the maximum wind speed, while only two models indicate a decrease. Although the MPI model predicts an increase in the number of extreme events, the maximum wind speed for this model decreases. As a general conclusion, one could conclude that there is no indication of an increase in the number of extreme events, but that the highest wind speeds could increase.

Table 2: The number of "extreme events" per year and the maximum wind speed at Westhinder for the different models and the historical and climate RCP 8.5 scenario simulations.

Model	Historical simulations		RCP 8.5 simulations		
	# extr.	Max. Ws	# extr.	Max. Ws	Diff # extr.
MEAS 1h	100.13	29.22			
MEAS 3h	56.93	28.69			
MEAS 6h	41.28	28.22			
ALARO	21.37	24.18	20.27	24.91	-1.10
CNRM	22.60	25.91	24.47	26.82	+1.87
COSMO	61.40	28.46	60.14	28.35	-1.26
ICHEC	31.16	27.34	27.57	28.37	-3.59
IPSL	16.90	22.17	17.80	22.76	+0.90
MOHC	29.23	24.61	27.50	26.45	-1.73
MPI	27.63	26.48	31.37	25.35	+3.74

In Figure 22, the maximum wind speed for a certain return period for the different models is shown, without the bias correction. While the number of extreme events is higher in the measurements than in the model results (except for the COSMO model), the maximum wind speed for a certain return period are more similar. However, it can be seen that most models predict higher maximum wind speeds in the climate RCP 8.5 simulation, than for the historical simulations.

As mentioned in the previous section, the cumulative distribution functions (CDF) of the historical run will be corrected, so that the cumulative distribution functions must have the same characteristics as the cumulative distribution

function of the measurements. The CDF of the climate run is corrected in the same way. An example is shown in Figure 23. One can see that the historical probability function is indeed corrected to the measurement function. The climate results are corrected accordingly.

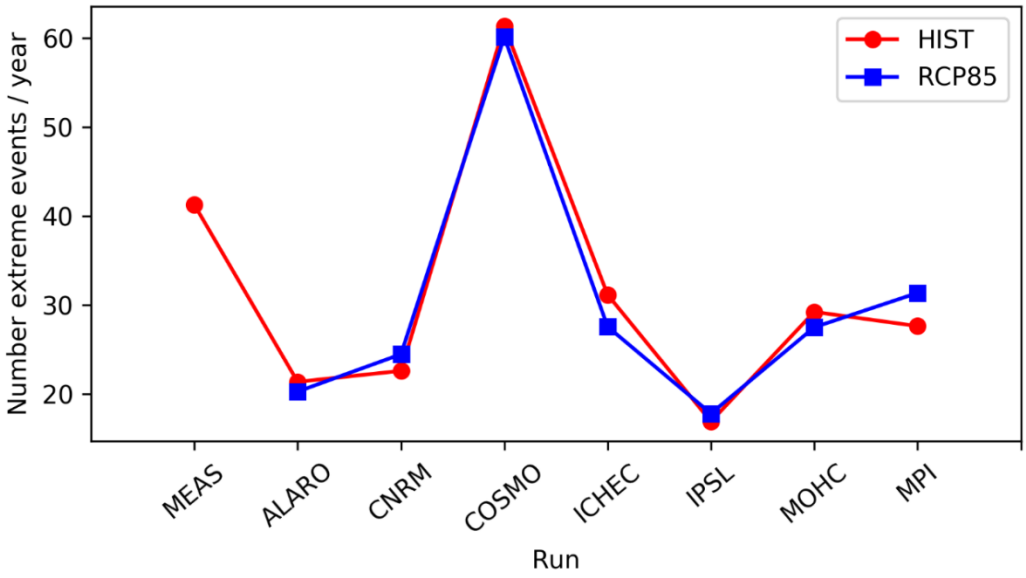

Figure 21: Number of extreme events per year for the wind speed, for the measurements (6h), and for the different models (historical and climate RCP 8.5 runs).

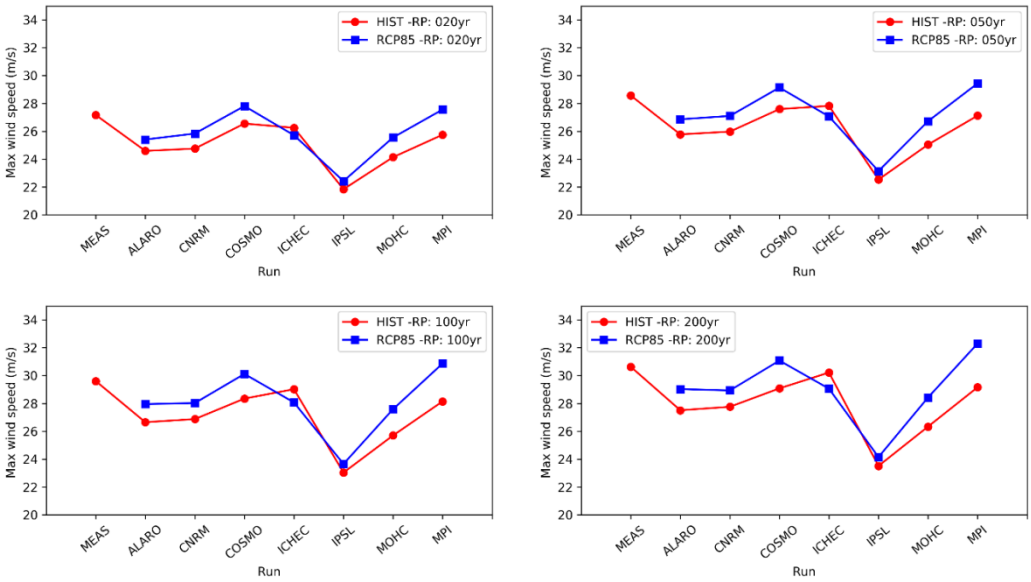

Figure 22: Non-corrected maximum wind speed for a certain return period, for the measurements (6h) and the different models (historical and the climate RCP8.5 simulations). Upper left/right, lower left/right: return period of 20, 50, 100 and 200 years.

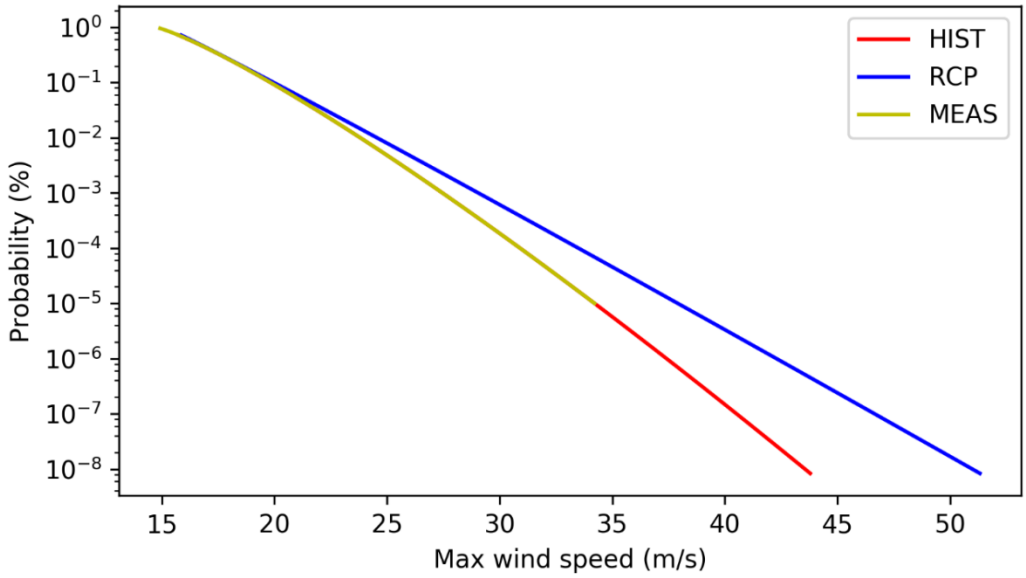

Figure 23: Corrected probability functions (logaritmic scale) for the measurements, the historical and the climate RCP8.5 simulations for the ALARO model.

In Figure 24, the corrected maximum wind speeds for different return periods are shown for the historical and the climate RCP8.5 simulations. Since the CDF for the historical runs were corrected, the maximum significant wave heights for the historical runs are the same as the one derived from the measurements. On the other hand, also the maximum wind speeds of the climate RCP8.5 runs were corrected. As for the uncorrected results, the maximum wind speed increases for all models, but for the ICHEC model. For the return period of 20 years, the maximum wind speed increase varies between +3% to +8.5%, while for the return period of 200 years, the increase is larger, up to +12% for the MPI model.

In Figure 25, the same information is given in a box plot, where for the different return periods the maximum wind speed is given for the measurements (left) and for the results of the climate simulations (right). The plot shows an increase in maximum wind speed, but with a rather large uncertainty. This is mainly due to the results of the ICHEC model, that predicts a decrease in maximum wind speed.

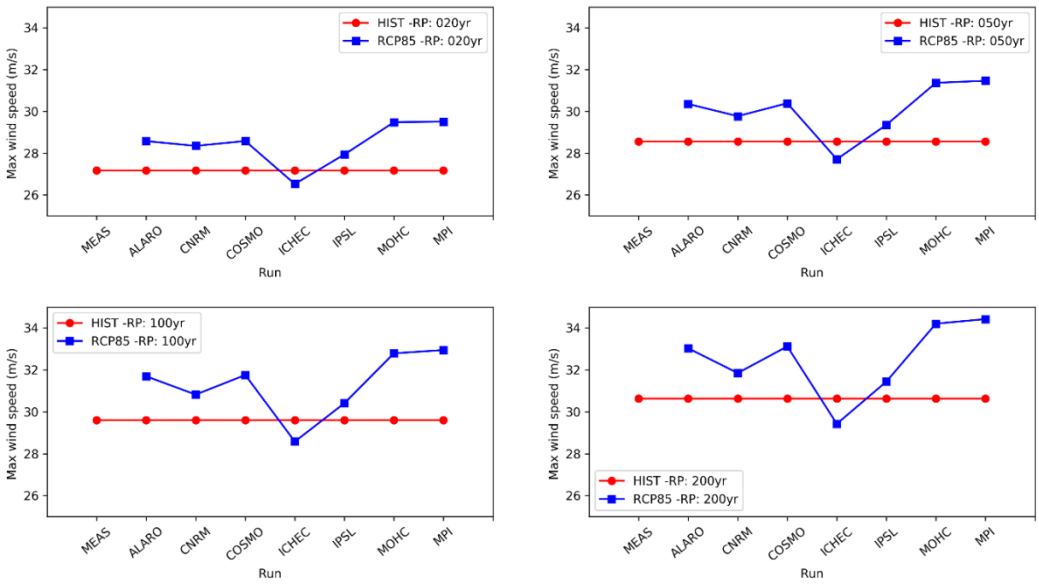

Figure 24: Corrected maximum wind speed for a certain return period, for the different models and for the historical and the climate RCP8.5 simulations. Upper left/right, lower left/right: return period of 20, 50, 100 and 200 years.

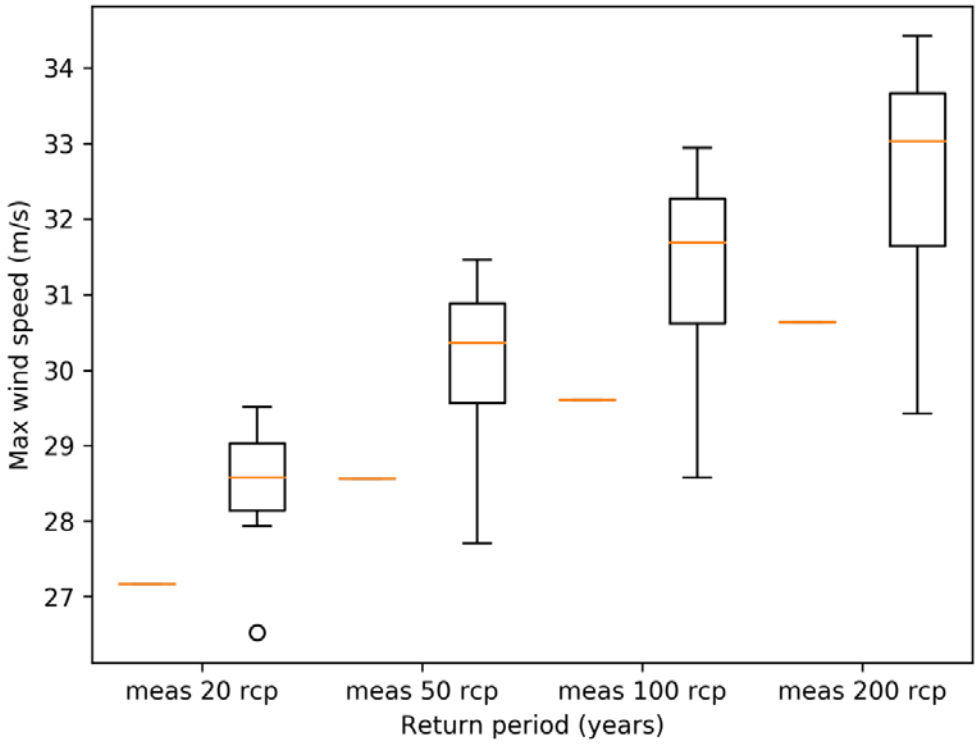

Figure 25: Box plot of the maximum wind speed with a certain return period (20, 50, 100 and 200 years). Left: results of measurements (and historical simulations), Right: results of the climate RCP8.5 simulations.

5. Analysis of significant wave heights

5.1. *Measurements at Bol van Heist*

The analysis of the changes in extreme significant wave heights due to climate changes on the Belgian coast is executed for the station Bol van Heist, near the harbour of Zeebrugge. Observations were obtained from the Meetnet Vlaamse Banken (Vlaamse Gemeenschap, Agentschap Maritieme Dienstverlening en Kust). The timeseries at Bol van Heist proved to be the longest timeseries of wave data available at the Belgian coast, covering data from March 1978 onwards. For the current study, data for the period 1978-2015 were used. Unfortunately, not the full period is available, since some data gaps were found. Furthermore, the data were not always available at the same temporal resolution. To have a uniform time series, which is also compatible with the model results, the measurements were averaged over a period of 3h, which is also the resolution of the output of the wave models. A total of 31.65 years of data was collected during the full period.

Extreme values were defined when the significant wave height was larger than 1.8 m, with an increment for the definition of the classes of 0.12 m. A total of 890 storms were found over a period of 31.65 years of data, with one storm with a maximum significant wave height between 3.48 m and 3.60 m

In Figure 26 and Figure 27, the probabilities and the Weibull distributions are shown for the measurements at Bol van Heist. In the last figure, the probabilities are given with a logarithmic scale. The maximum significant wave height is relatively low. This is mainly due to the fact that the measurements are averaged over 3 h timespan. Extreme values during these three hours are filtered out. This needs to be taken into account when analyzing the results.

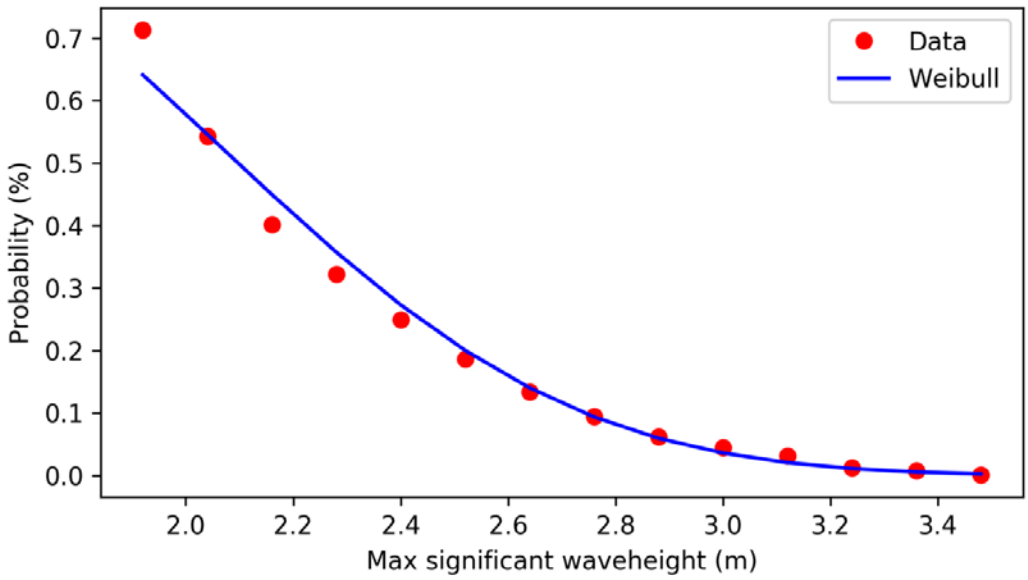

Figure 26: Probability that during a storm a certain significant wave height is reached in the measurements at Bol van Heist.

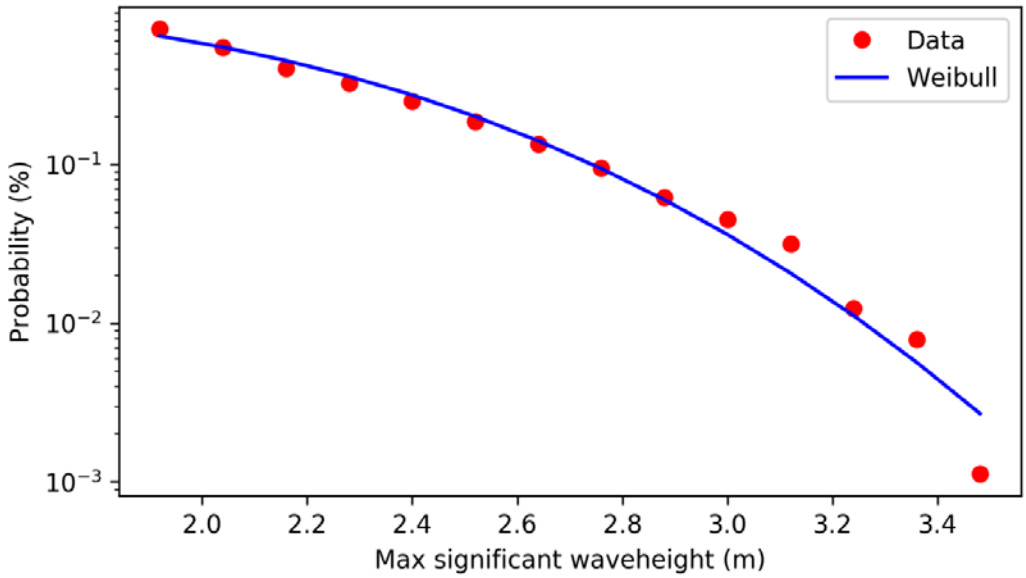

Figure 27: Probability (logaritmic distribution) that during a storm a certain significant wave height is reached in the measurements at Bol van Heist.

Furthermore, remind this is the Weibull distribution that will be matched with the Weibull distributions calculated using the historical simulations and that the same correction, using the quantile mapping method, will be used to correct the results of the climate simulations. These corrected distributions will then be used to calculate the wave heights with a certain return period.

5.2. *Analysis of the model results*

In Table 3 the number of "extreme" event (significant wave height higher than 1.8 m) is given together with the maximum significant wave height calculated during the period. First of all, it is seen that the number of storms varies between 14 storms for the IPSL model to 38 storms for the COSMO model, but that they are on average around 28 storms per year. It can be seen however that there is no increase of the number of events in the RCP 8.5. Five models indicate that the number of storms will decrease in the climate simulations, while only two models (CNRM and MPI) indicate a moderate increase in the number of storms. This information is also shown in Figure 28.

Four models also see a decrease in the maximum significant wave height found over the 30 year period, while three models indicate an increase. Also the COSMO model, in addition to the CNRM and the MPI models, indicate an increase in maximum significant wave height.

In Figure 29 the maximum significant wave height for a certain return period for the different models is shown, without the bias correction. It is clear that the results of the model give higher wave heights than the measurements. Only the results of IPSL model give similar wave heights. Furthermore, it can be seen that for five models, the wave heights for a certain return period in the climate RCP8.5 simulations are lower than for the historical simulations, indicating a decrease in

extreme waves in the future climate. The COSMO and the CNRM models however, indicate higher extreme waves in the future.

Table 3: The number of "extreme events" and the maximum significant wave height at Bol van Heist for the different models and the historical and climate RCP 8.5 scenario simulations.

Model	Historical simulations		RCP 8.5 simulations		
	# storms	Max. Hs	# storms	Max. Hs	Diff # storms
MEAS	28.12	3.48 m			
ALARO	20.70	5.45 m	20.27	5.03 m	-0.43
CNRM	24.17	4.70 m	26.81	5.52 m	+2.64
COSMO	37.57	5.10 m	35.40	5.77 m	-2.17
ICHEC	31.77	4.99 m	25.83	4.72 m	-5.94
IPSL	14.87	4.16 m	14.13	3.92 m	-0.74
MOHC	27.27	5.29 m	26.43	4.78 m	-0.84
MPI	28.20	4.63 m	29.40	4.72 m	+1.20

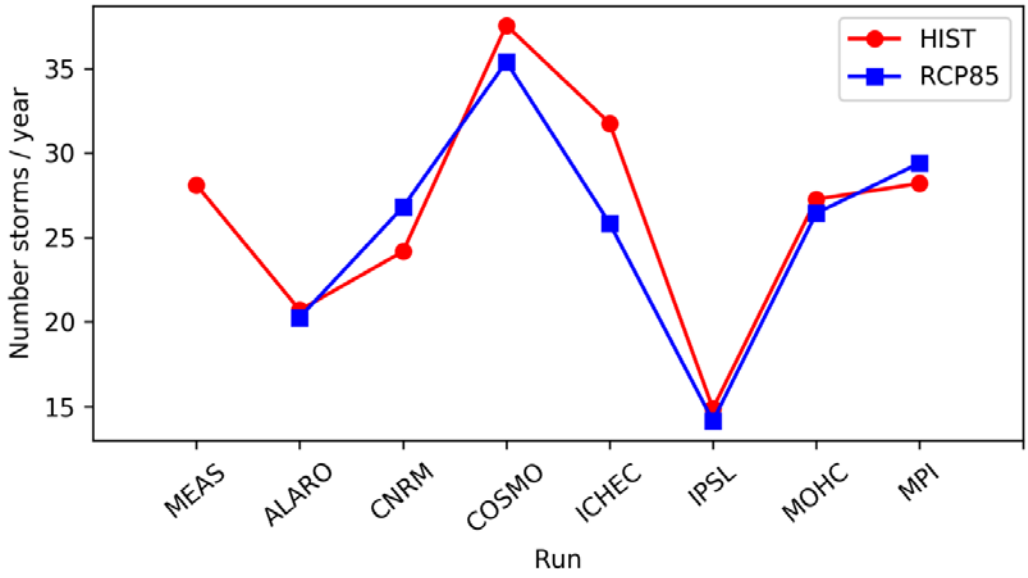

Figure 28: Number of storms per year for the different models and for the historical and climate RCP 8.5 runs.

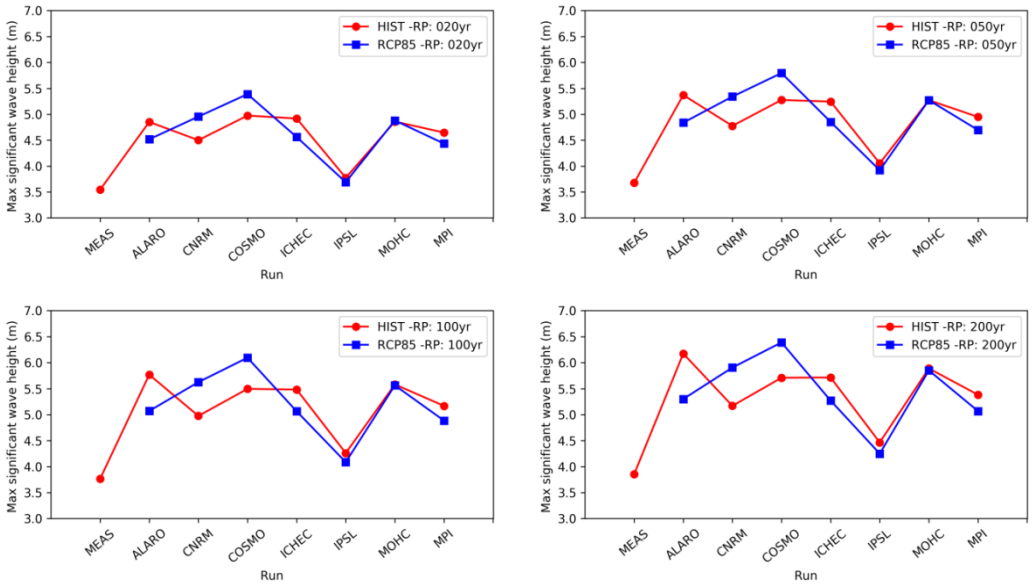

Figure 29: Non-corrected maximum significant wave height for a certain return period, for the different models and for the historical and the climate RCP8.5 simulations. Upper left/right, lower left/right: return period of 20, 50, 100 and 200 years.

As mentioned already, the cumulative distribution functions (CDF) of the historical run will be corrected, so that the cumulative distribution function is having the same characteristics as the cumulative distribution function of the measurements. The CDF of the climate run is corrected in the same way. An example is shown in Figure 30. One can see that the historical probability function is indeed corrected to the measurement function. The climate results are corrected accordingly.

In Figure 31 the corrected maximum significant wave heights for different return periods are shown for the historical and the climate RCP8.5 simulations. Since the CDF for the historical runs were corrected, the maximum significant wave heights for the historical runs are the same as the one derived from the measurements. On the other hand, also the maximum significant wave heights of the climate RCP8.5 runs were corrected. It can be seen that the changes compared to the measurements are now relatively small. For three models (CNRM, COSMO en MOHC), a small increase is predicted, while for the four other models, no change or a small decrease are expected. In Figure 32, the same information is given in a box plot, where for the different return periods the maximum significant wave height is given for the measurements (left) and for the results of the climate simulations (right). The plot shows that for the return periods of 20 and 50 years, a small increase in maximum significant wave height could be expected, while for the longer return periods, no changes are to be expected. The plot also shows however that some uncertainty in the results still exists.

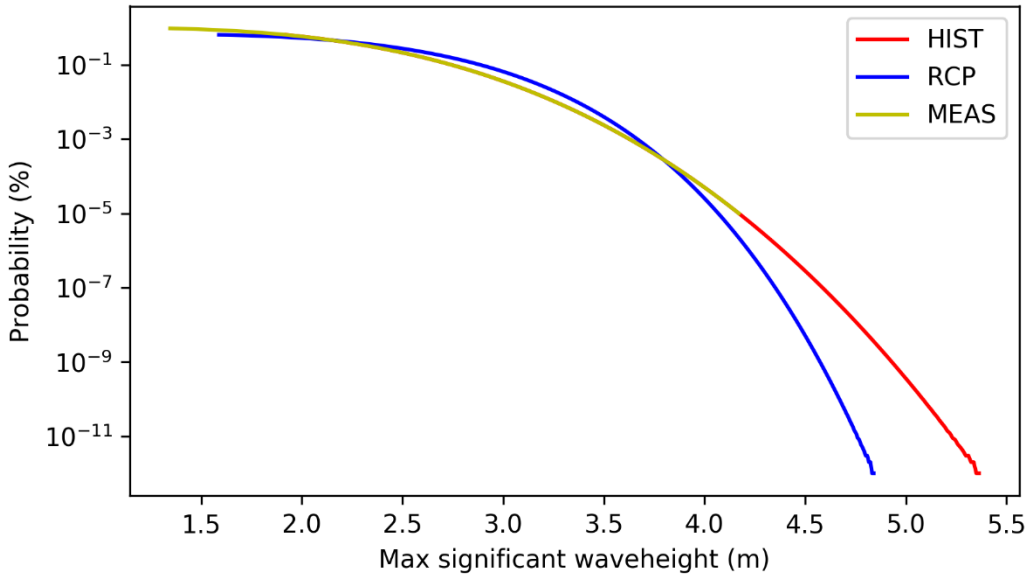

Figure 30: Corrected probability functions (logaritmic scale) for the measurements, the historical and the climate RCP8.5 simulations for the ALARO model.

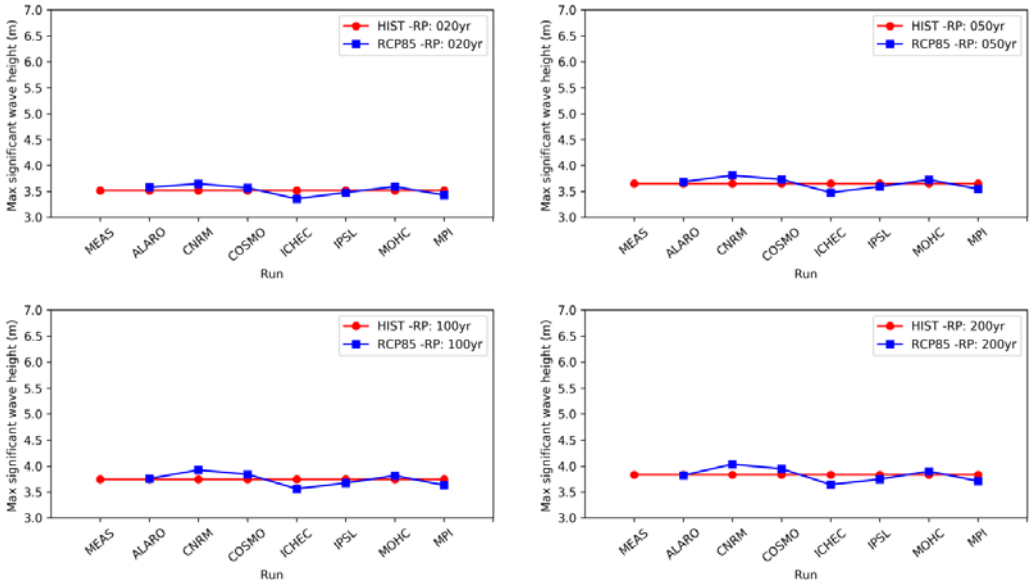

Figure 31: Corrected maximum significant wave height for a certain return period, for the different models and for the historical and the climate RCP8.5 simulations. Upper left/right, lower left/right: return period of 20, 50, 100 and 200 years.

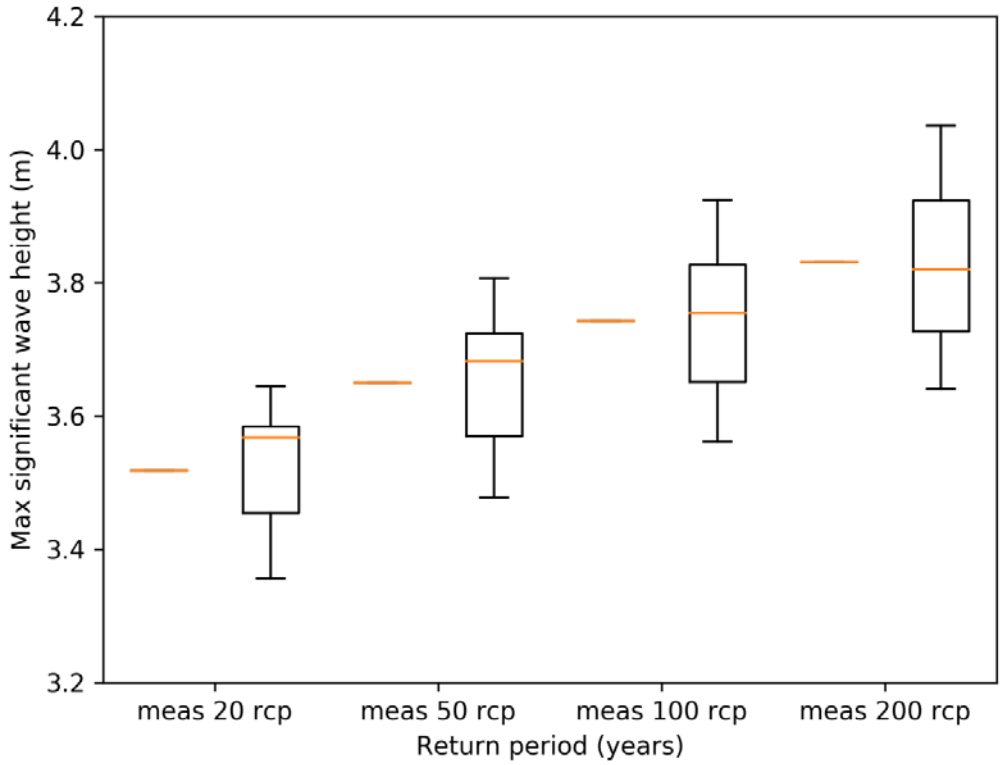

Figure 32: Box plot of the maximum significant wave height with a certain return period (20, 50, 100 and 200 years). Left: results of measurements (and historical simulations), right: results of the climate RCP8.5 simulations.

6. Analysis of storm surges

6.1. *Measurements at Ostend*

The analysis of the changes in storm surges due to climate changes on the Belgian coast is executed for the station Ostend. Observations were obtained from the Meetnet Vlaamse Banken (Vlaamse Gemeenschap, Agentschap Maritieme Dienstverlening en Kust). The timeseries at Ostend was the longest timeseries of water elevation data available at the Belgian coast, covering data from 1980 to 2006, with a time interval of 1h. Longer time series are available, but only the high waters and the low waters were available at the moment for older data. Also more recent data are available, but these data were not fully quality checked for now. Therefore, the data for the period 1980-2006 were used in this study, covering a period of 27 years. To calculate the 'measured' storm surges the time series of the calculated time series of the water elevation at Ostend, without taking the meteorological conditions into account, are substracted from the measured water elevations.

Extreme values were in this case defined when the storm surge was larger than 0.5 m, with an increment for the definition of the classes of 0.05 m. A total of 2356 extreme events were found over a period of 27 years of data, with one extreme event with a maximum storm surge between 2.30 m and 2.35 m.

In Figure 33 and Figure 34, the probabilities and the Weibull distributions are shown for the measurements of the storm surge in Ostend. In the last figure, the probabilities are given with a logarithmic scale. In this figure, it can be seen that one very high extreme value occurs with a storm surge higher that 2.30 m.

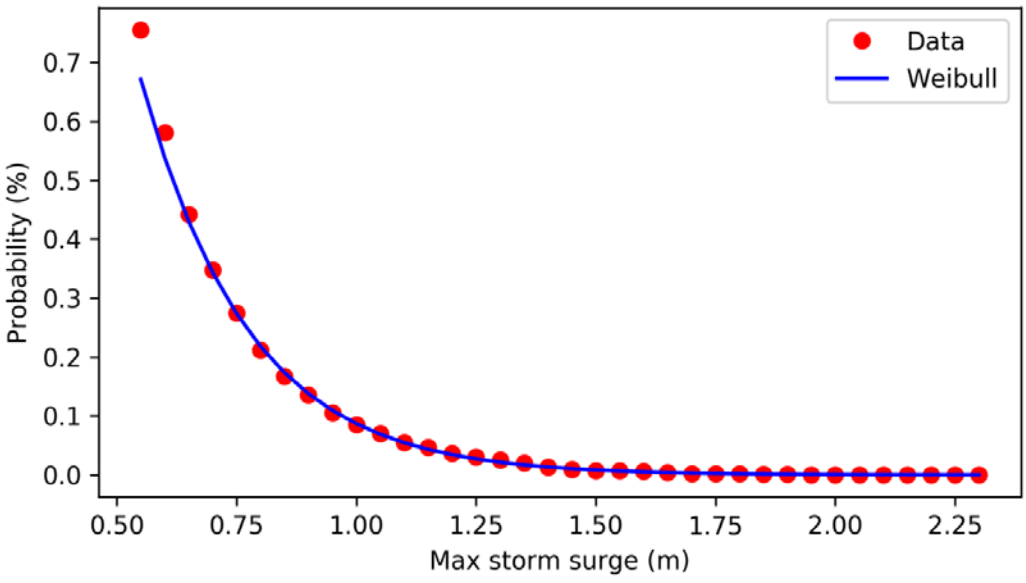

Figure 33: Probability that during a storm a certain surge elevation is reached in the measurements at Ostend.

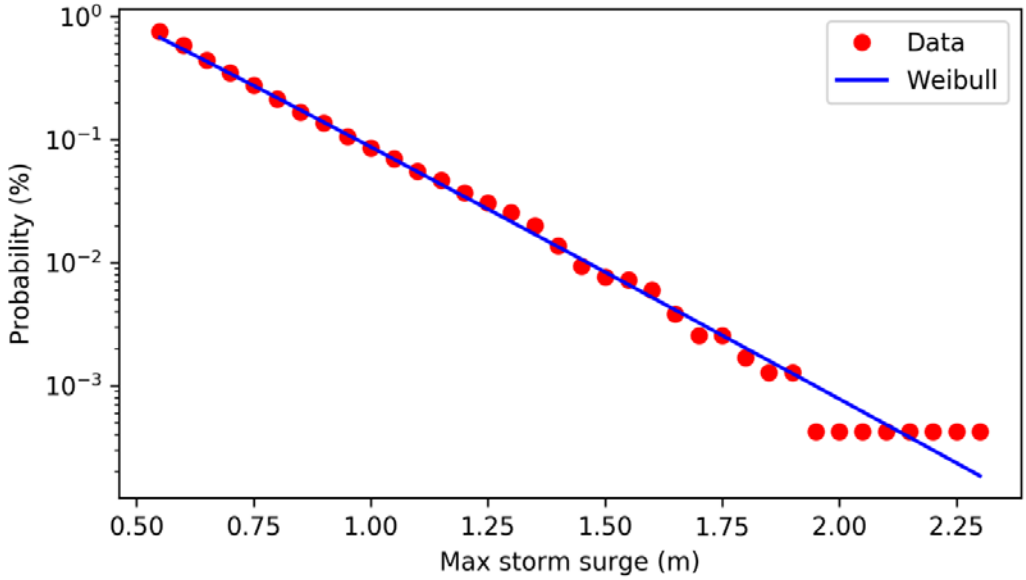

Figure 34: Probability (logaritmic distribution) that during a storm a certain storm surge is reached in the measurements at Ostend.

6.2. *Analysis of the model results*

In Table 4, the number of "extreme" events (storm surge higher than 0.5 m) is given together with the highest storm surge observed during the period. First of all, the number of extreme events in the measurements is clearly higher than in the model results. This can be seen in Figure 35. Furthermore, the number of extreme events is similar in the historical simulations as in the climate simulations. Only for the ICHEC and the MOHC models, the number of extreme events is clearly lower for the climate runs, while it is larger for the CNRM and MPI models. However, it is clear from the table that in this case, the maximum storm surge found for the entire period is higher in the climate runs, than for the historical runs. The average over the seven models is increasing from 2.22 m to 2.35 m, an increase with more than 5 %. Only for the IPSL model, the maximum storm surge in the climate run is smaller than the maximum in the historical run.

In Figure 36, the maximum storm surge for a certain return period for the different models is shown, without the bias correction. This is more a function of all extreme events over the entire period, and not only a result of the maximum storm surge, encountered during the period. For the MOHC and the MPI models, the maximum expected storm surges for a certain return period is larger for the climate simulations, while these maximum expected storm surges are smaller for the ICHEC and IPSL models. For the ALARO, COSMO and CNRM models, the maximum storm surges are similar. Furthermore, it is clear that the maximum storm surge in the observations is much more in line with the model results, than for the number of extreme events.

Table 4: The number of "extreme events" and the maximum significant wave height at Bol van Heist for the different models and the historical and climate RCP 8.5 scenario simulations.

Model	Historical simulations		RCP 8.5 simulations		
	# storms	Max. surge	# storms	Max. surge	Diff # storms
MEAS	87.26	2.35 m			
ALARO	30.10	2.27 m	30.73	2.38 m	+0.63
CNRM	43.80	2.07 m	46.50	2.36 m	+2.70
COSMO	51.40	2.26 m	49.77	2.35 m	-1.63
ICHEC	64.16	2.17 m	56.20	2.32 m	-7.96
IPSL	54.23	2.40 m	56.40	2.18 m	+2.17
MOHC	55.33	2.36 m	50.27	2.46 m	-5.06
MPI	54.00	2.02 m	57.97	2.37 m	+3.97

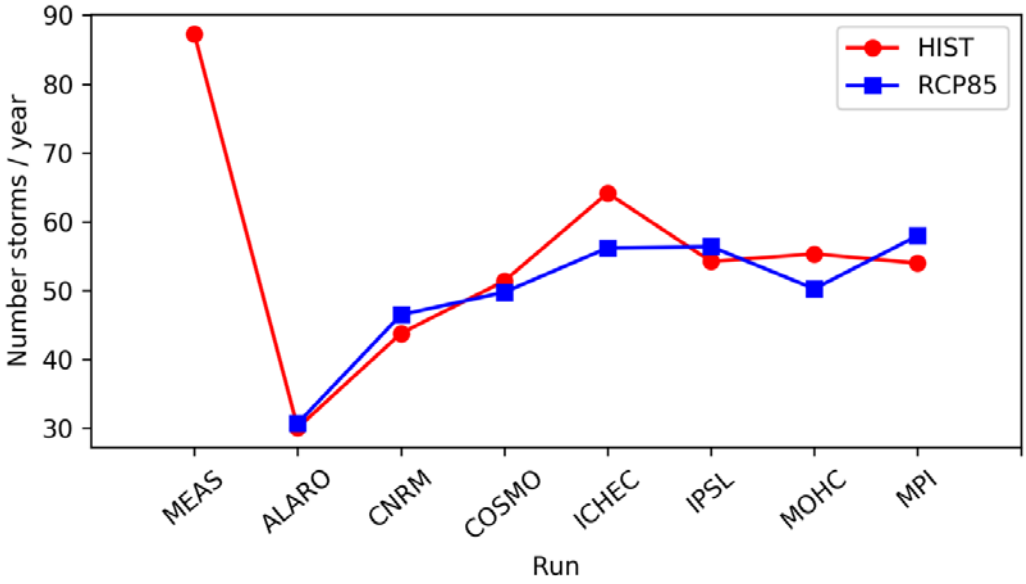

Figure 35: Number of extreme events per year for the different models and for the historical and climate RCP 8.5 runs.

As before, the Weibull distributions will be quantile corrected. In the corrected storm surges for different return periods are shown for the historical and the climate RCP8.5 simulations. Since the CDF for the historical runs were corrected, the maximum storm surges for the historical runs are the same as the one derived from the measurements. On the other hand, also the maximum storm surges of the climate RCP8.5 runs were corrected. The changes compared to the measurements are now relatively small. For the MPI model a larger increase in storm surges is predicted, while for the CNRM and MOHC, the increase remains limited. For the IPSL and the ICHEC model, a decrease is predicted, which is more important forth IPSL model.

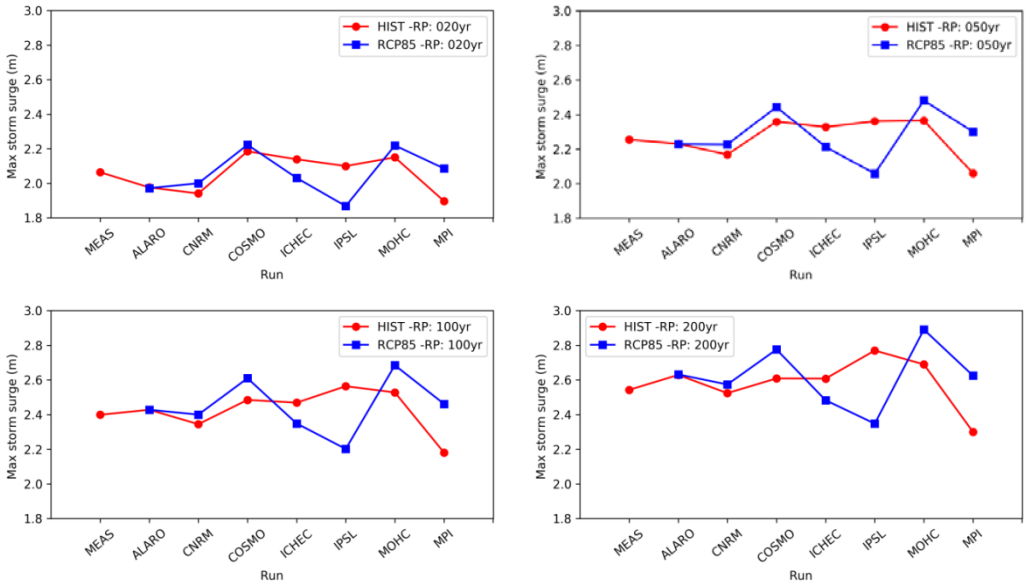

Figure 36: Non-corrected maximum storm surge for a certain return period, for the different models and for the historical and the climate RCP8.5 simulations. Upper left/right, lower left/right: return period of 20, 50, 100 and 200 years.

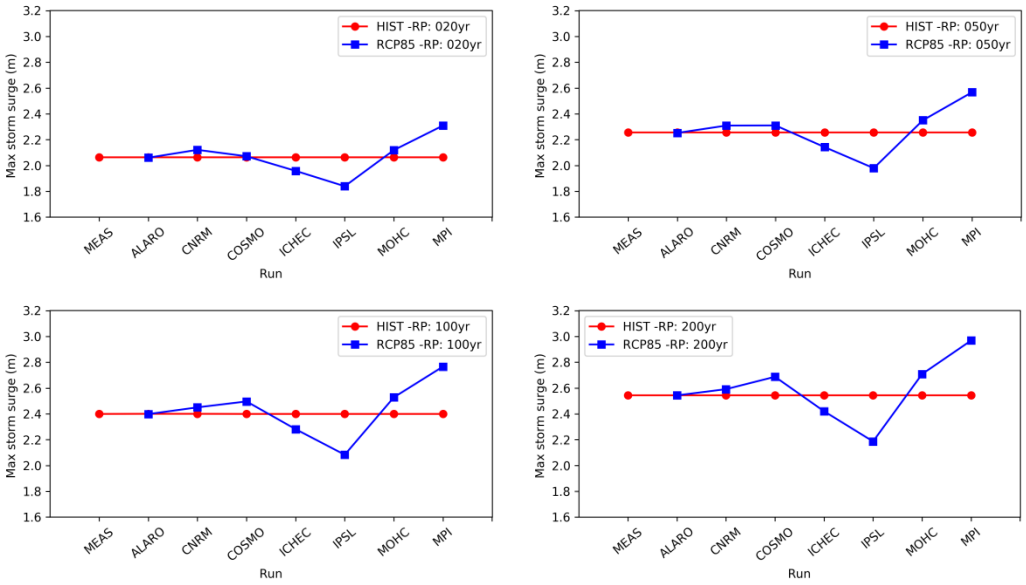

Figure 37: Corrected maximum storm surge for a certain return period, for the different models and for the historical and the climate RCP8.5 simulations. Upper left/right, lower left/right: return period of 20, 50, 100 and 200 years.

In Figure 38, the same information is given in a box plot, where for the different return periods the maximum storm surge is given for the measurements (left) and for the results of the climate simulations (right). The plot shows that for the return periods of 20 and 50 years, a small increase in storm surge could be expected, while for the longer return periods, no changes are to be expected. The plot also shows that the uncertainty in the results remains important.

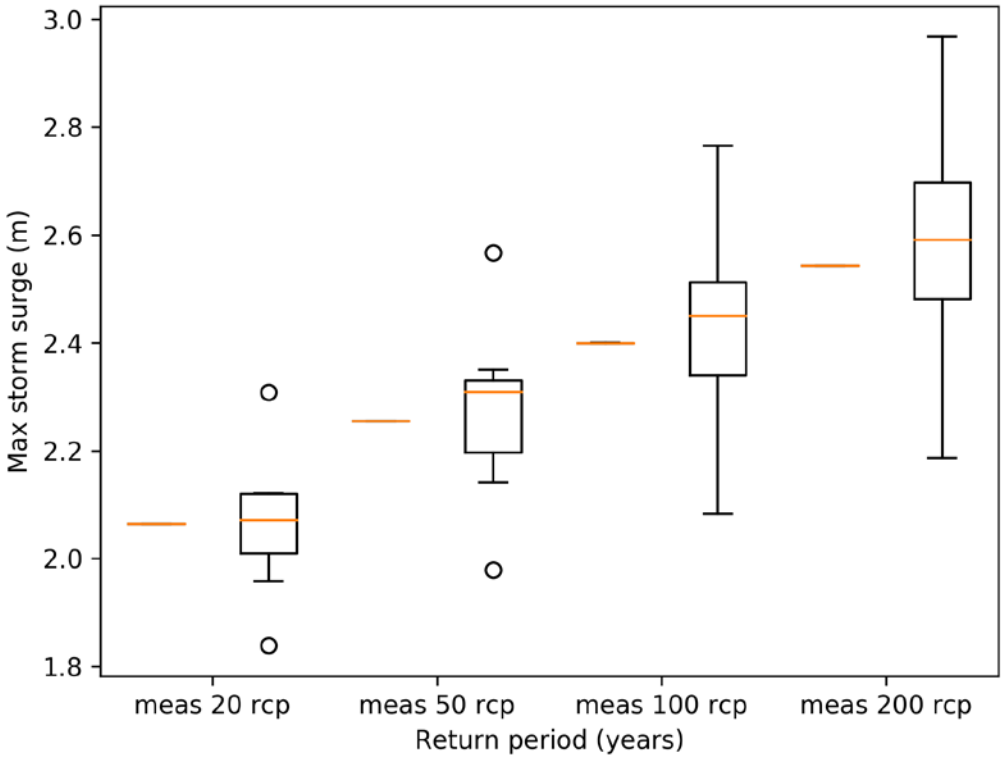

Figure 38: Box plot of the storm surge with a certain return period (20, 50, 100 and 200 years). Left: results of measurements (and historical simulations), right: results of the climate RCP8.5 simulations.

7. Discussion

The main conclusions from the analysis is that for the Belgian coast, it seems that we could expect some increase in high wind speeds, but that no increase in extreme waves and storm surges are to be expected. These seems in at first sight contradictory. However, this could be explained by a change in wind direction, a quite low correlation between extreme events in winds, waves and surges, and by the fact that the extreme waves and the extreme surges are mainly induced by wind speeds blowing to the southeast. These are discussed in the next sections.

7.1. Change in wind direction

In Figure 40 the wind roses are presented for the ALARO model, for the historical and the climate runs. No big differences are seen. From the wind roses, we can calculate also the 'overall mean wind speed' and wind direction over the period. These are represented in Figure 41. One can see that overall, a small change in wind direction occurred, from winds towards NE (south-westerly winds) to winds towards NEE, an anti-clockwise shift of around -7°. A similar change in wind direction can be found in the other models, see Figure 42. For the ALARO, COSMO, CNRM and MPI models, an anti-clockwise shift to more westerly winds between -10° and -5° is found, while for the other models, the shift is less important. Remark that the shift in direction is certainly not uniform over the model grid. The same calculation of the change in wind direction was done also for three other (arbitrary chosen) station over the grid, which are given in Figure 39.

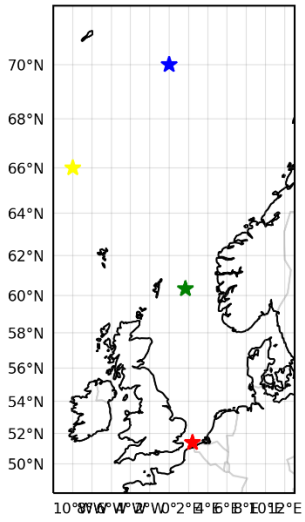

Figure 39: Position of Westhinder (red), North (blue), West (yellow) and Northeast (green) stations.

One can see in Figure 42, that for the other stations, different changes in wind direction can be observed. Furthermore, the difference between the different models are again quite large, certainly for the station West.

Since the extreme events in wave height and storm surge are most of the time generated by higher wind speeds, the same exercise was calculated for the high

winds, higher than 20 m/s. Without showing the wind roses and the mean wind speeds, the change in wind direction is shown in Figure 43. The different models again can give quite different results.

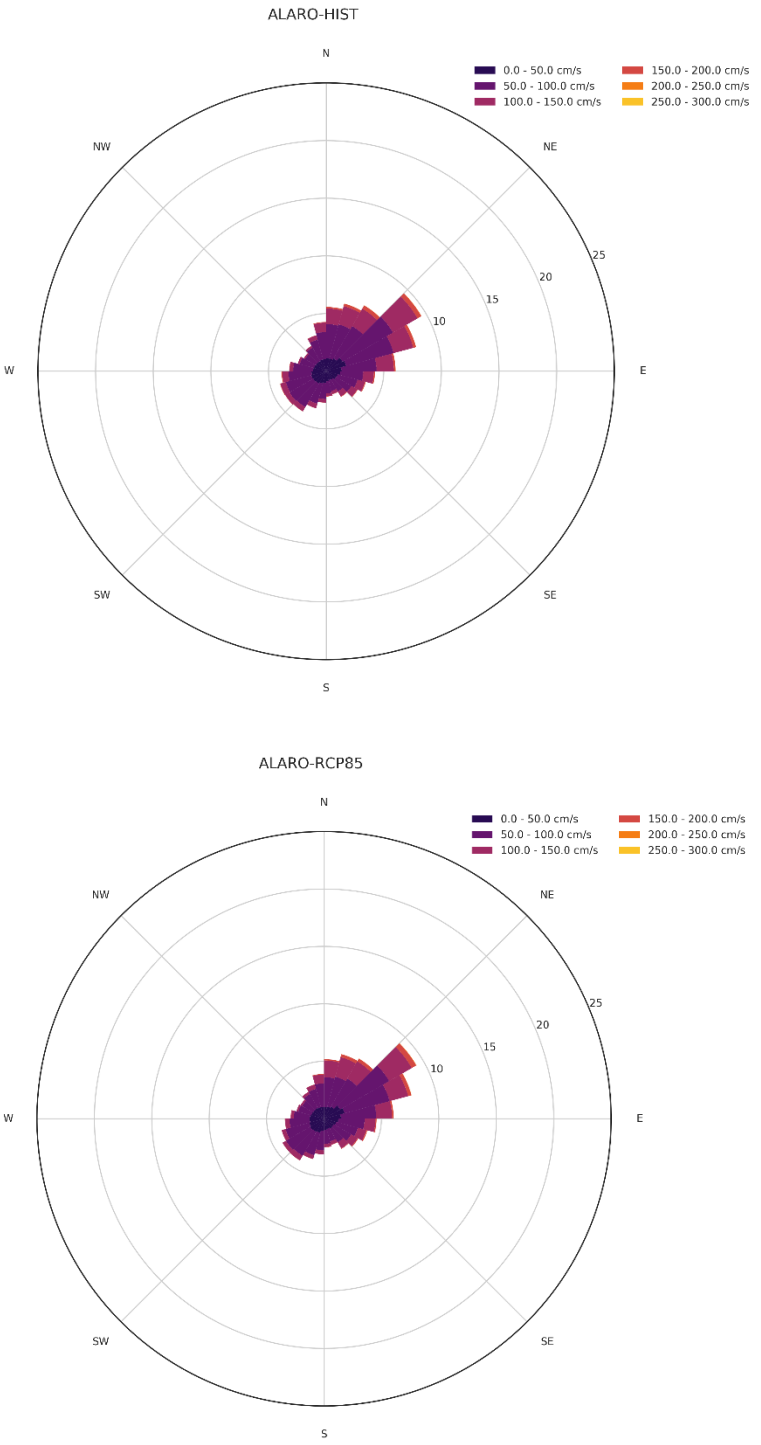

Figure 40: Wind roses for the ALARO model at Westhinder for the historical (above) and climate RCP85 (below) runs.

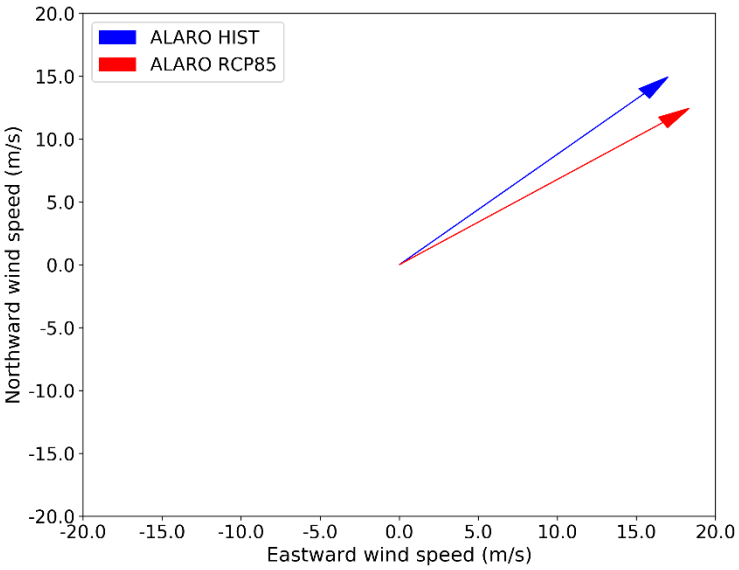

Figure 41: Overall mean wind speed and wind direction for the ALARO wind at Westhinder, for the historical and the climate RCP85 run.

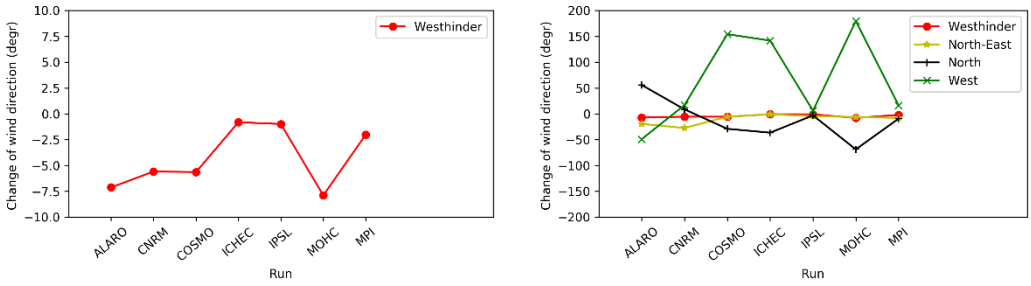

Figure 42: Change in wind direction for the different models at Westhinder (left) and for the different stations (right). Shift is RCP-HIST. Negative is anti-clockwise.

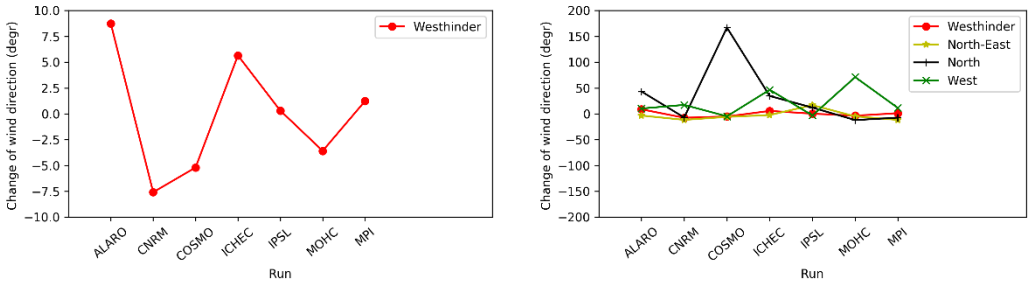

Figure 43: Change in wind direction for the different models at Westhinder (left) and for the different stations (right) for wind speeds higher than 20 m/s.). Shift is RCP-HIST. Negative is anti-clockwise.

7.2. *Correlation between extremes for winds, surges and waves*

A second indicator that higher wind speeds are not necessary an indication for higher waves and/or higher surges is that there is a relatively low coincidence between the extreme events for the winds and surges and for the winds. This is for instance indicated in Figure 44. In this figure for the top 250 extreme events for the waves, surges and wind speeds for the Belgian coast, it was checked whether a top 250 extreme events for the waves was also a top 250 extreme events for the surges and for the wind speed. It was seen that ALARO model and for the historical run, only for 72 events, a top extreme event for the waves was also an extreme event for the surges and for the wind speed. For the other models and the other simulations, similar values were found. Furthermore, it can be seen in the figure, that in different cases a high wave doesn't coincide with a high wind speed are vice/versa.

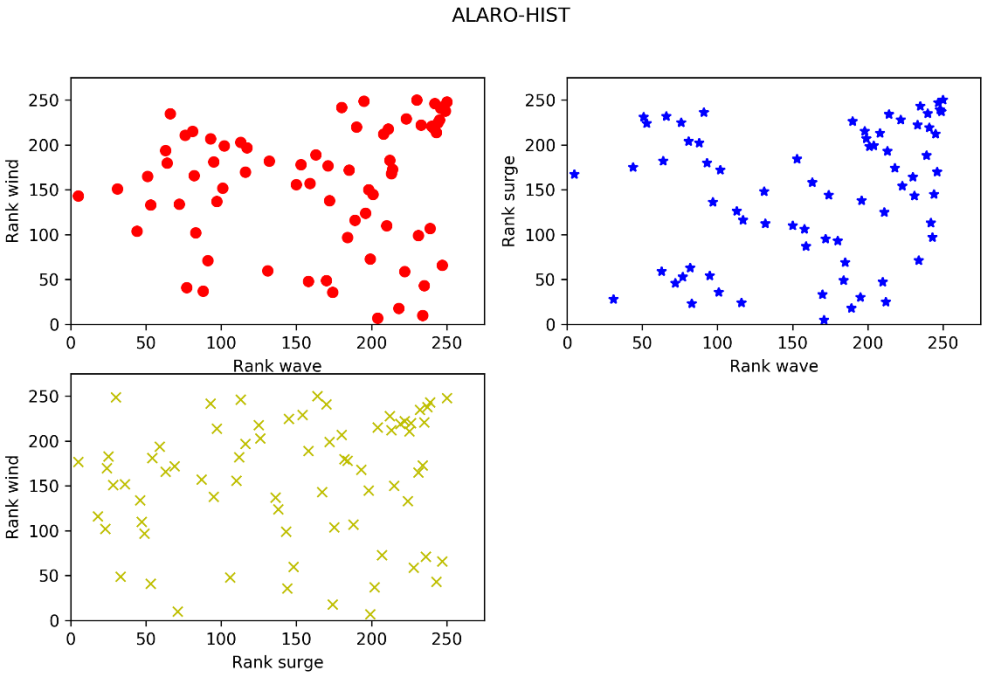

Figure 44: Relation between the top 250 extreme events for the waves, surges and wind speed for the ALARO historical simulation.

Remark further that also the correlation between the high waves and high surges is not higher. This is again an indication that extreme wind speeds at the Belgian coast itself is not necessary imply extreme waves and/or extreme storm surges. Also the wind direction and the duration of the event are of importance, amongst probably other factors.

7.3. *Relation between extreme waves, surges and winds, and wind direction*

Finally, it is clear that there is a relation between the extreme waves and extreme surges and the wind directions. This is also shown again for the ALARO model and the historical run, in Figure 45. One can observe that the very high significant wave heights and the very high storm surges are indeed correlated with higher wind speeds. For lower significant wave heights and storm surges, wind speeds could be lower or higher, dependent on the wind direction.

Furthermore, the most extreme wave heights and storm surges are related to winds blowing coming from the north or north-west. This is of course the waves with the longest fetches are the winds blowing the water to the shore, and thus generating higher storm surges. Therefore, strong winds coming from the north to north-west are the winds, with the most severe waves and storm surges. In Figure 46 for the ALARO, COSMO and ICHEC models, the linear regression is shown for the historical runs and the climate RCP85 runs, between the wind speed and the wind directions. The highest wind speeds are wind speeds coming from north to north-east. Furthermore, it can be seen that for the climate RCP85 runs, the higher wind speeds are more turned to the north-east than to the north, indicating a slight anti-clockwise shift in the direction of high wind speeds (see Figure 47). This means that in the climate RCP85 runs, higher wind speeds have less chance to come from the north-west, creating higher waves and storm surges.

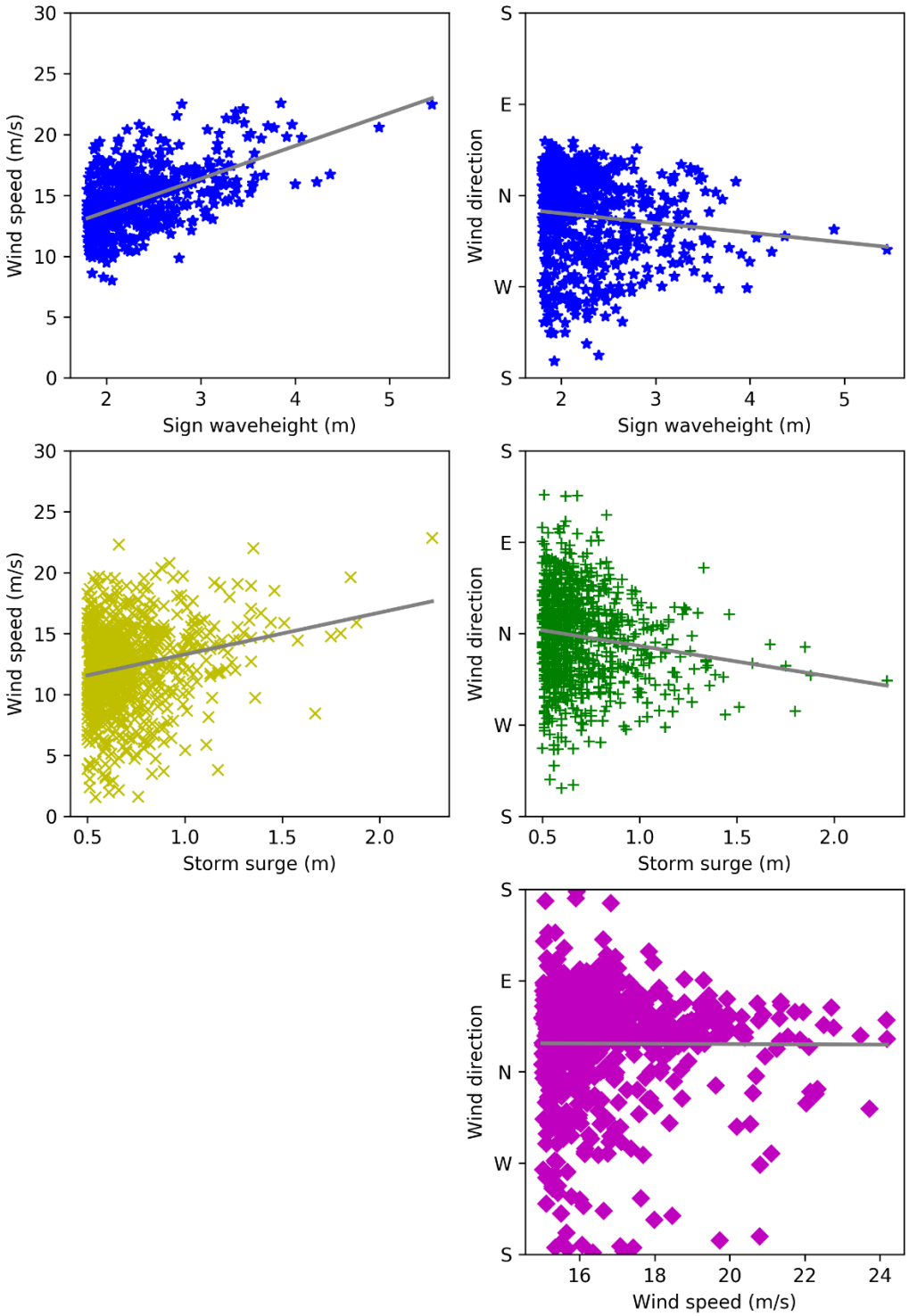

Figure 45: Relation between extreme wave height, extreme storm surge and extreme wind speed, with the wind direction for the ALARO model and the historical run. (Wind direction = direction where wind is coming from).

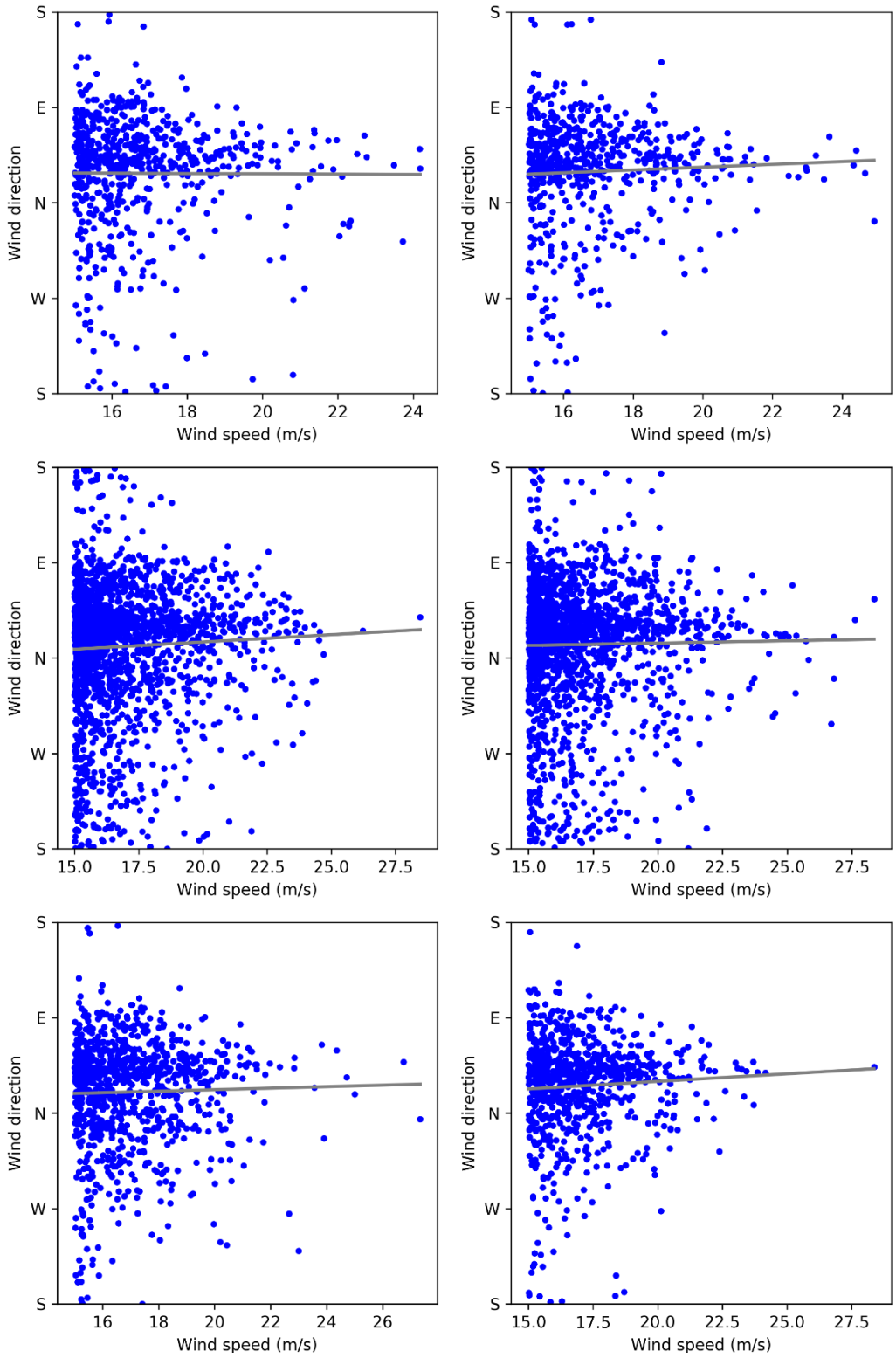

Figure 46: Relation between high wind speed and wind direction for ALARO (top), COSMO (middle) and ICHEC (lower) models and for the historical runs (left) and climate RCP85 runs (right). Wind direction = direction where wind is coming from.

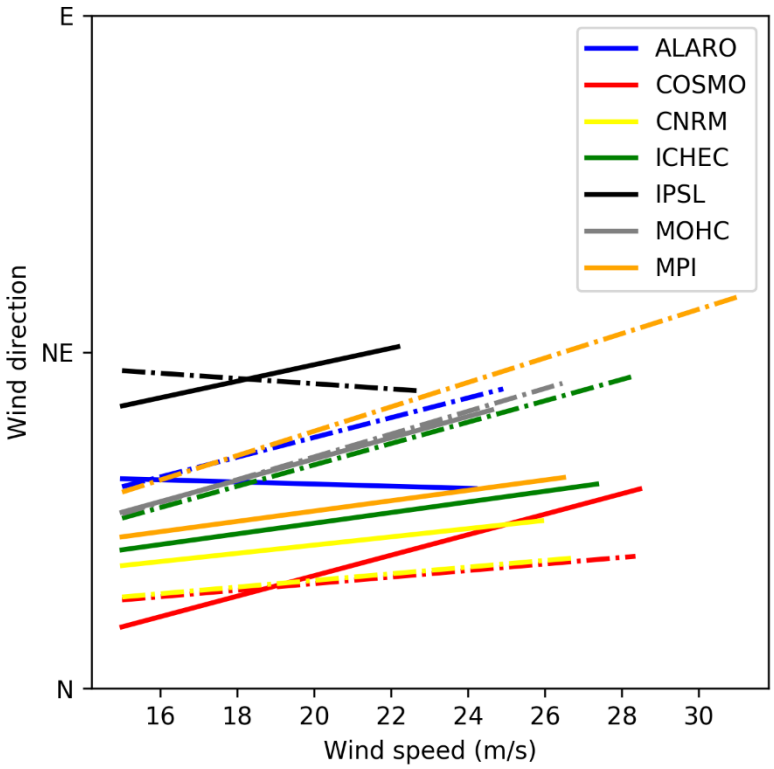

Figure 47: Linear regression for the relation between high wind speeds and wind directions, for the different models: full lines, historical runs; dashed lines: climate RCP85 runs.

7.4. *Conclusions*

A clear and obvious reason for the expected increase in wind speed, while there is no expected increase in extreme waves and storm surges, is not straightforward to assess. In this section, it has been shown that changes in wind directions are occurring, both for the overall wind speed at the Belgian coast (station Westhinder) and for the high wind speeds. While the overall wind speed could turn clockwise, it has been shown that the higher wind speeds, an anti-clockwise change in direction from north to north-east could be expected in the models. This could explain why higher wind speeds could be expected, with no increase in expected waves and surges.

Furthermore, it has been shown that in different regions of the North Sea, different behaviour and changes in wind speed and wind direction could be expected. More research on this is necessary and is in preparation (Ponsar *et al.*, in preparation).

Finally, it has to be stressed that there still is much variability in the models results and that also the calculation of the Weibull distribution, based on a linear regression, could have an influence on the results of the research.

8. Conclusions

In this report, some results are presented on the research on the impact of changing meteorological conditions on the extreme wind speed, significant wave height and storm surges at the Belgian coast. Seven results of regional atmospheric models were obtained in the framework of the CORDEX.be Brain.be project or were downloaded from the CORDEX website. All models cover the North-west European Continental Shelf with a resolution of about 12.5 km and a time resolution of at least 6h. A 30-year period covering the current climate (historical run) and a 30-year period, covering the last 30 years of the 21th century, assuming the IPCC RCP8.5 scenario, were studied. A two-dimensional hydrodynamic model COHERENS, was used to calculate the storm surges, while a third-generation WAM model, was used to calculate the waves.

The study focused on the extreme events and used a Weibull distribution to parametrise the probability distribution functions and to calculate the return periods for a certain level (of wave height, wind speed or storm surge). A bias-correction method, based on quantile mapping, was used to correct the model results for the bias, and to map the historical runs results with the measurements that were available.

The research showed to for the extreme wind speeds, some increase could be expected due to climate change. Although a large variability exists in the model results, most models indicate an increase in high wind speeds. This is however not the case for the extreme wave heights and the extreme storm surges. Here not significant changes are to be expected. One must however take into account also here the large variability in the model results.

A first attempt has been made to explain why the wind speeds are expected to increase, while this is not the case for the waves and the storm surges. One of the main reasons that could be found is the fact that for the higher wind speeds, an anti-clockwise change in direction from north to north-east could be expected in the models.

9. Acknowledgements

The research was executed in the framework of the CREST project. Part of the preparating work was already done in the BRAIN.be CORDEX.be project. Piet Termonia and Bert Van Schaeybroeck are gratefully acknowledged for making the ALARO wind fields from the Royal Meteorological Institute available. Prof. N. Van Lipzig from the Catholic University of Leuven is gratefully acknowledged for making the COSMO wind fields available for our research. The data from the other models were downloaded from the CORDEX data base. The Flemish Government, Agentschap Maritieme Dienstverlening en Kust, is thanked for making the measurements data available. Sieglien De Roo from the Flemish Hydraulics Research is thanked for making the long-term wave data at Westhinder available for this research. Prof. Patrick Willems (Catholic University Leuven) is thanked for his input on bias correction methods. Colleagues from the Flemish Hydraulics Research are thanked for their constructive input during a workshop.

10. References

Devis A., N.P.M. van Lipzig and M. Demuzere, 2018. Should future wind speed changes be taken into account in wind farm development? Environmental Research Letters, 13, 6, 064012. doi: 10.1088/1748-9326/aabff7.

Giot, O., P. Termonia, D. Degrauwe, R. De Troch, S. Caluwaerts, G. Smet, J. Berckmans, A. Deckmyn, L. De Cruz, P. De Meutter, A. Duerinckx, L. Gerard, R. Hamdi, J. Van den Bergh, M. Van Ginderachter and B. Van Schaeybroeck, 2016. Validation of the ALARO-0 model within the EURO-CORDEX framework. Geoscientific Model Development, 9, 1143-1152. doi: 10.5194/gmd-9-1143-2016.

Günther, H., S. Hasselmann and P.A.E.M. Janssen, 1992. Wamodel Cycle 4. DKRZ Technical Report No. 4, Hamburg, October 1992, 102 pp.

Fang, G.H., J. Yang, Y.N. Chen and C. Zammit, 2015. Comparing bias correction methods in downscaling meteorological variables for a hydrologic impact study in an arid area in China. Hydrology and Earth System Sciences, 19, 2547-2559, doi: 10.5194/hess-19-2547-2015.

Helsen, S., S. Caluwaerts, L. De Cruz, M. Demuzere, R. De Troch, R. Hamdi, P. Termonia, S. Vanden Broucke, N.P. M. Van Lipzig, B. Van Schaeybroeck, H. Wouters, 2019. Consistent scale-dependency of future increases in hourly extreme precipitation in two 2 different convection-permitting models. Submitted to Climate Dynamics.

Kamphuis, J. William, 2010. Introduction to coastal engineering and management, 2nd edition. Advances Series on Ocean Engineering, Volume 30, World Scientific, Singapore, 525 pp.

Luyten, P. (editor), 2016. Coherens – A coupled hydrodynamic-ecological model for regional and shelf seas: user documentation. Version 2.6. RBINS Report, Operational Directorate Natural Environment, Royal Belgian Institute of Natural Sciences, Brussels, Belgium, 1554 pp.

Ozer, J., D. Van den Eynde and K. Baetens, 2017. Coherens New Common Setup: Validation of CoS + Validation of CoS – December storm. Presentation, Royal Belgian Institute of Natural Sciences.

Termonia, P., B. Van Schaeybroeck, L. De Cruz, R. De Troch, S. Caluwaerts, O. Giot, R. Hamdi, S. Vannitsem, F. Duchêne, P. Willems, H. Tabari, E. Van Uytven, P. Hosseinzadehtalaei, N. Van Lipzig, H. Wouters, S. Vanden Broucke, J.-P. van Yperseele, P. Marbaix, C. Villanueva-Birriel, X. Fettweis, C. Wyard, C. Scholzen, S. Doutreloup, K. De Ridder, A. Gobin, D. Lauwaert, T. Stravrakou, M. Bauwens, J.-F. Müller, P. Luyten, S. Ponsar, D. Van den Eynde and E. Pottiaux. 2018. The CORDEX.be initiative as a foundation for climate services in Belgium. Climate Services, 11, 49-61. doi: 10.1016/ j.cliser.2018.05.001.

Vanden Broucke, S., H. Wouters, M. Demuzere and N.P.M. van Lipzig, 2018. The influence of convection-permitting regional climate modeling on future projections of extreme precipitation:l dependency on topography and timescale. Climate Dynamics. doi: 10.1007/s00382-018-4454-2.

Van den Eynde, D., 2013. Comparison of the results of the operational HYPAS and WAM models. Report OPTOS/1/DVDE/201303/EN/TR1, Royal Belgican Institute for Natural Sciences, Operational Directorate Natural Environment,

Brussels, Belgium, 39 pp.

Van den Eynde, D., R. De Sutter, L. De Smet, F. Francken, J. Haelters, F. Maes, E. Malfait, J. Ozer, H. Pollet, S. Ponsar, J. Reyns, K. Van der Biest, E. Vanderperren, T. Verwaest, A. Volkaert and M. Willekens, 2011. Evaluation of climate change impacts and adaptation responses for marine activities "CLIMAR", Final Report, Brussels. Belgian Science Policy Office, Research Programme Science for a Sustainable Development, 121 pp.

The WAMDI Group, 1988. The WAM Model – A Third Generation Ocean Wave Prediction Model. Journal of Physical Oceanography, 18, 1775-1810.

11. Annex 1: Systematic and unsystematic RMSE

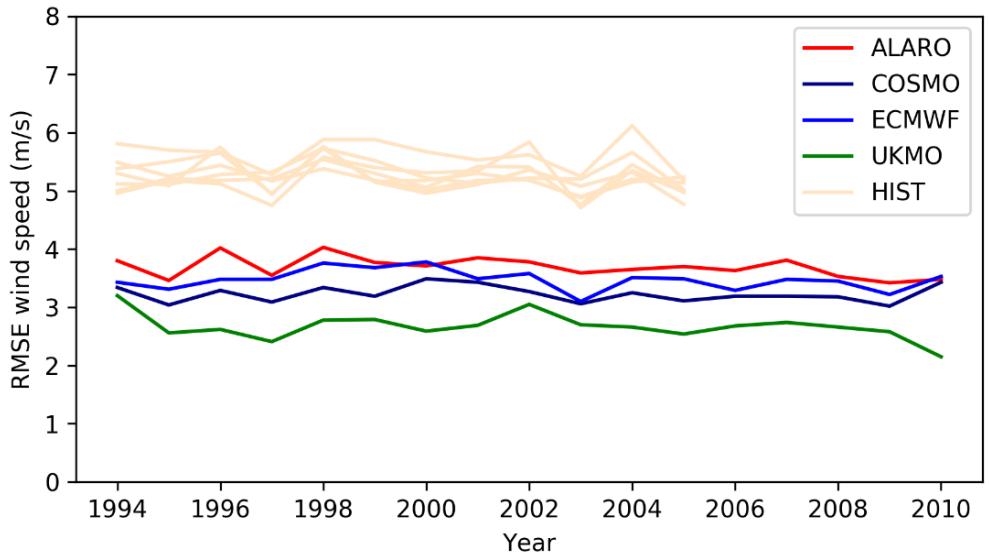

Figure 48: RMSE between the evaluation runs results for the ALARO, COSMO, ECMWF and UKMO data sets and the measurements at Westhinder.

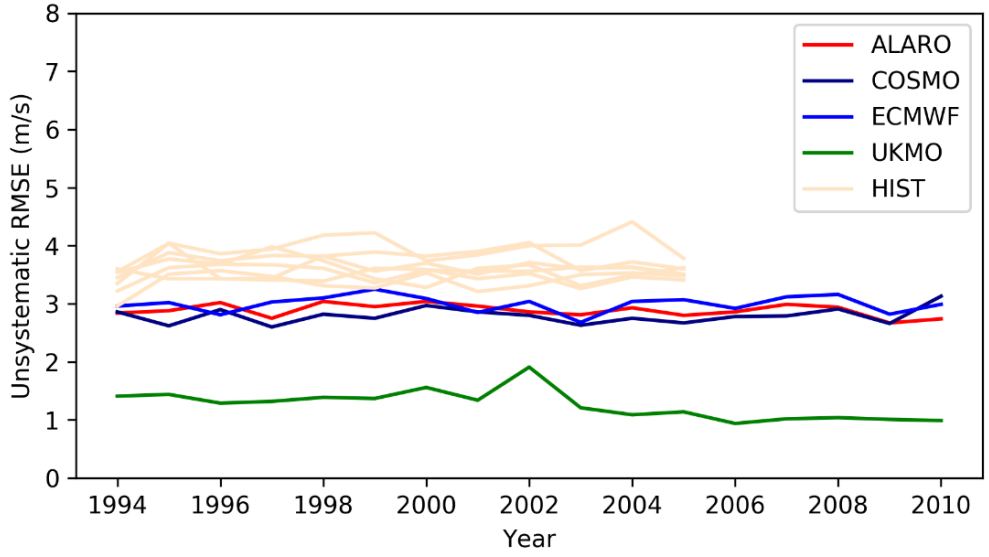

Figure 49: Unsystematic RMSE between the evaluation runs results for the ALARO, COSMO, ECMWF and UKMO data sets and the measurements at Westhinder.

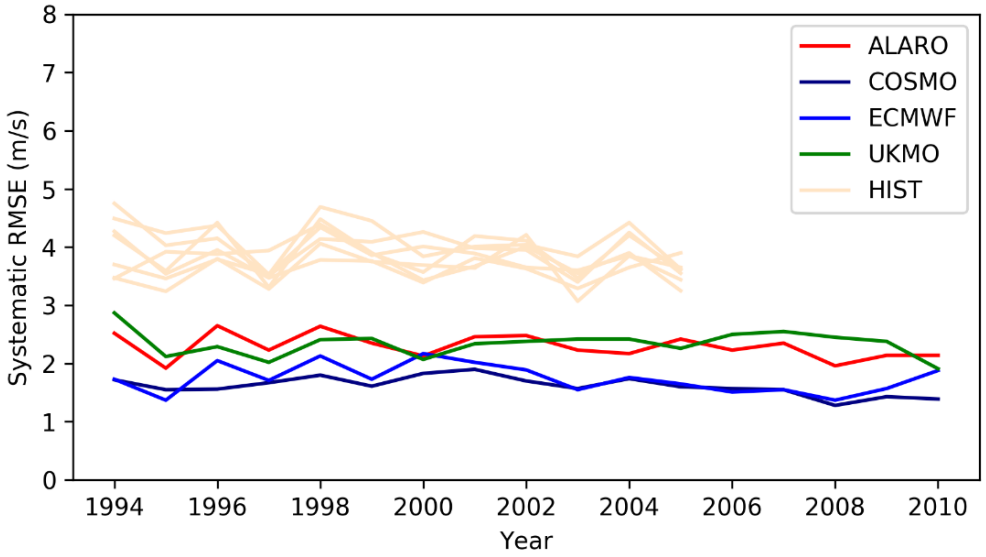

Figure 50: Systematic RMSE between the evaluation runs results for the ALARO, COSMO, ECMWF and UKMO data sets and the measurements at Westhinder.

12. Annex 2: Mean wind speed and standard deviation

12.1. Evaluation runs

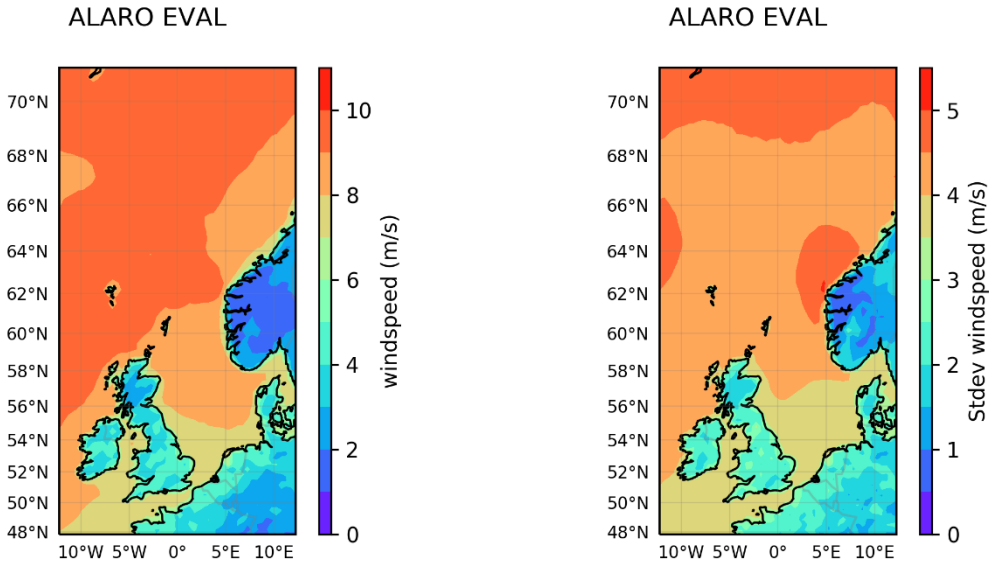

Figure 51: Mean wind speed map and standard deviation for ALARO

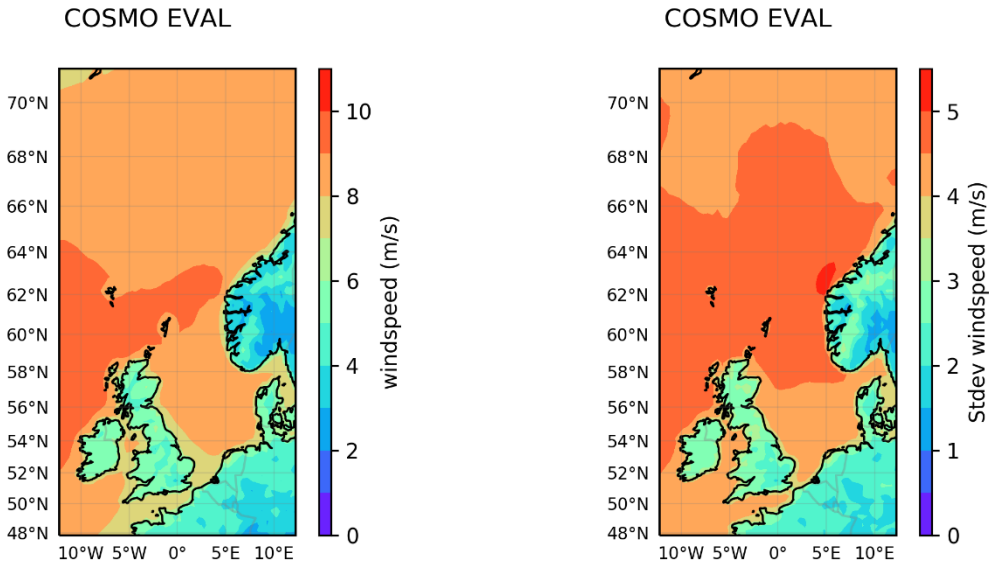

Figure 52: Mean wind speed map and standard deviation for COSMO

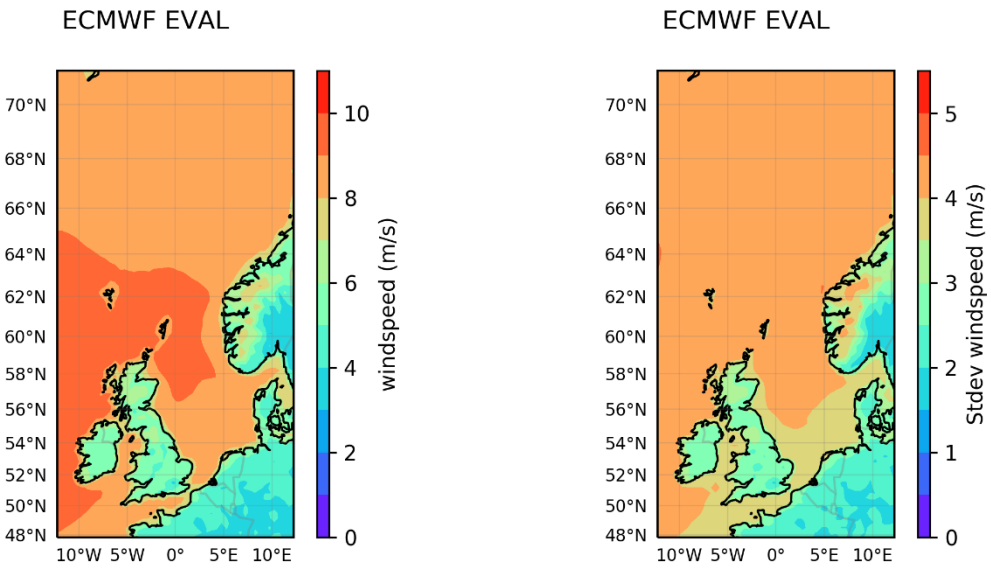

Figure 53: Mean wind speed map and standard deviation for ECMWF

12.2. Historical runs

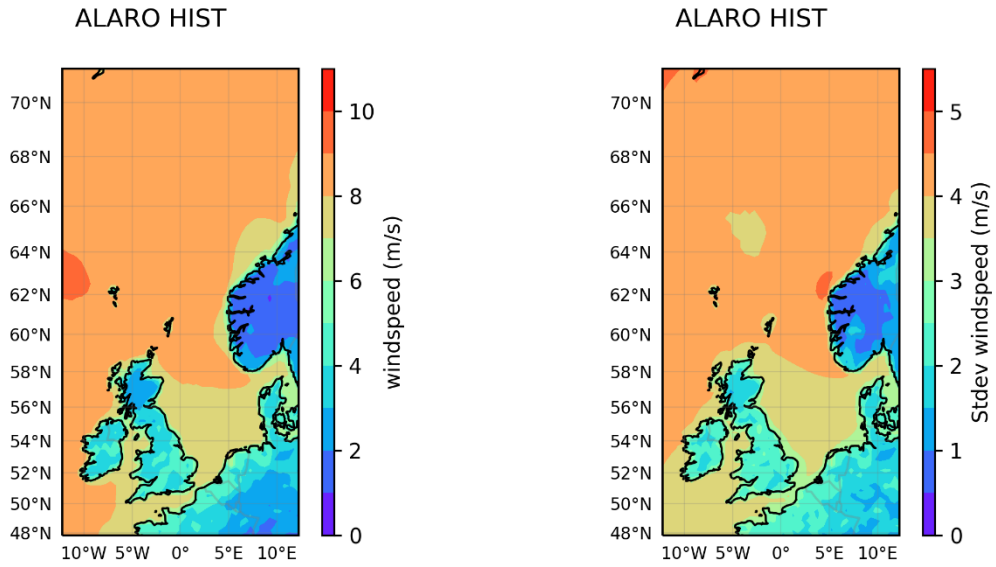

Figure 54: Mean wind speed map and standard deviation for ALARO

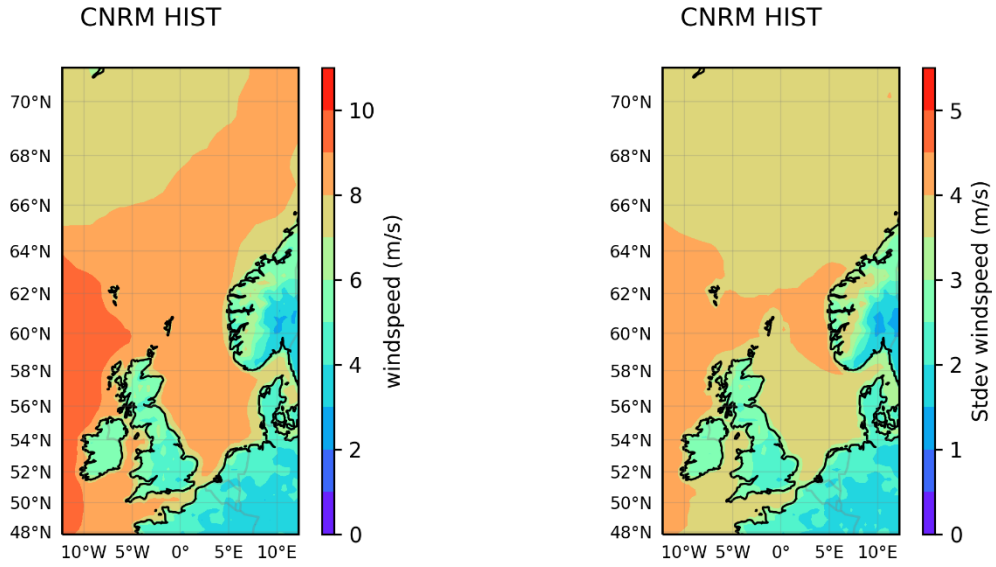

Figure 55: Mean wind speed map and standard deviation for CNRM

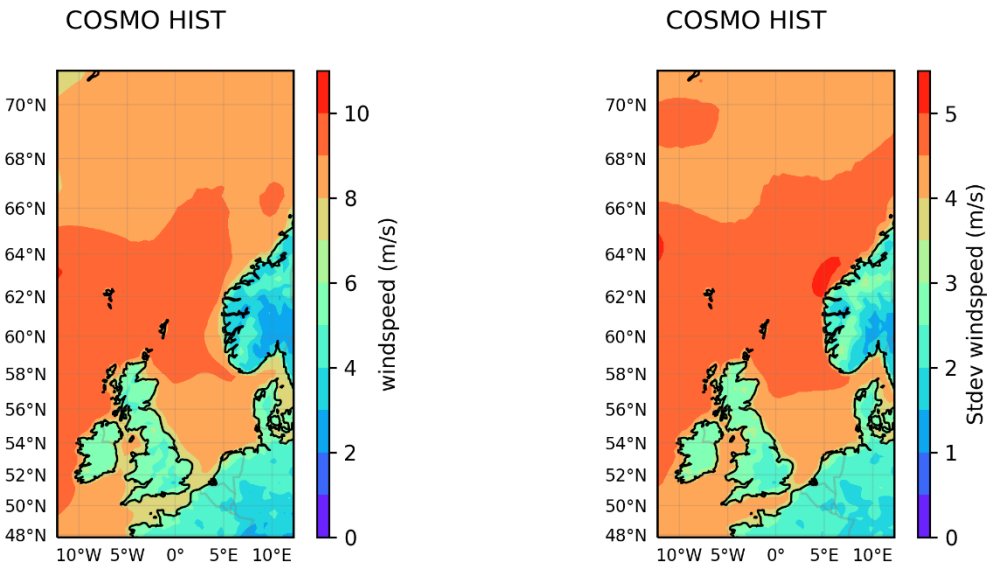

Figure 56: Mean wind speed map and standard deviation for COSMO

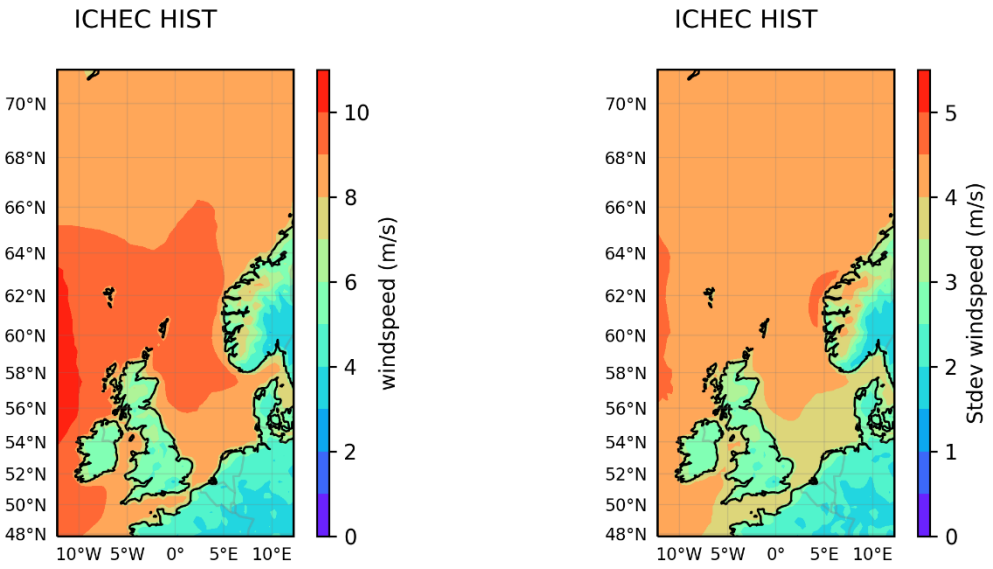

Figure 57: Mean wind speed map and standard deviation for ICHEC

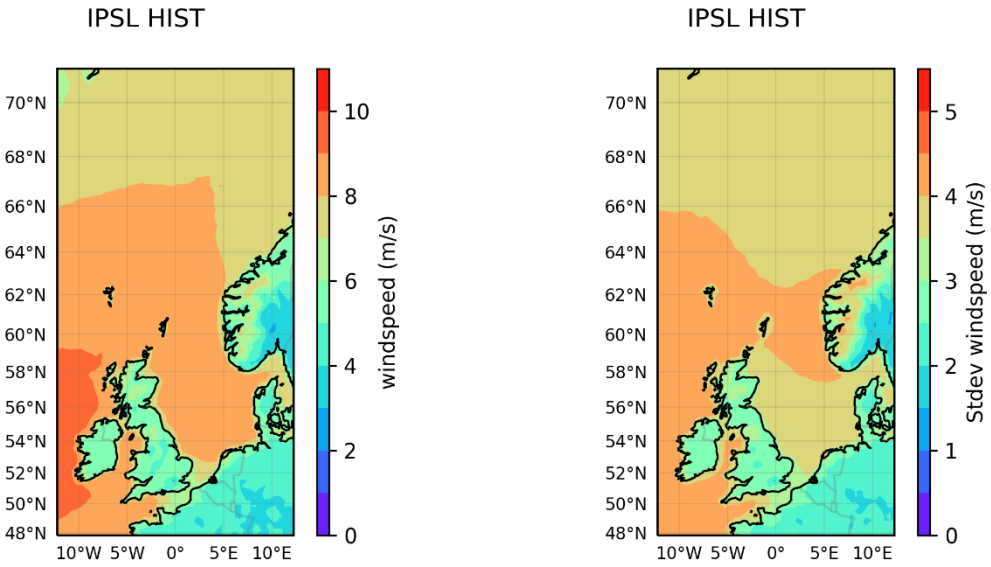

Figure 58: Mean wind speed map and standard deviation for IPSL

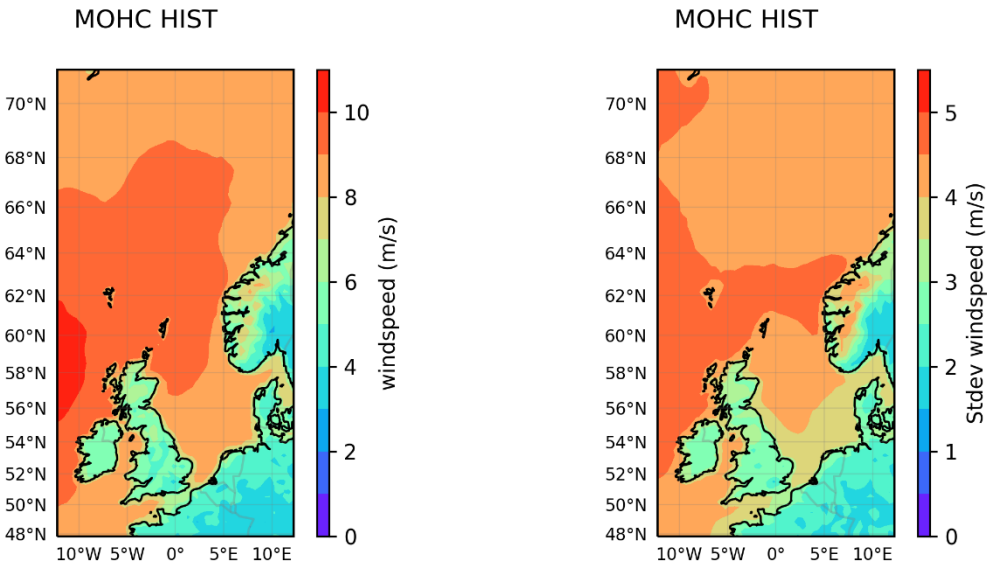

Figure 59: Mean wind speed map and standard deviation for MOHC

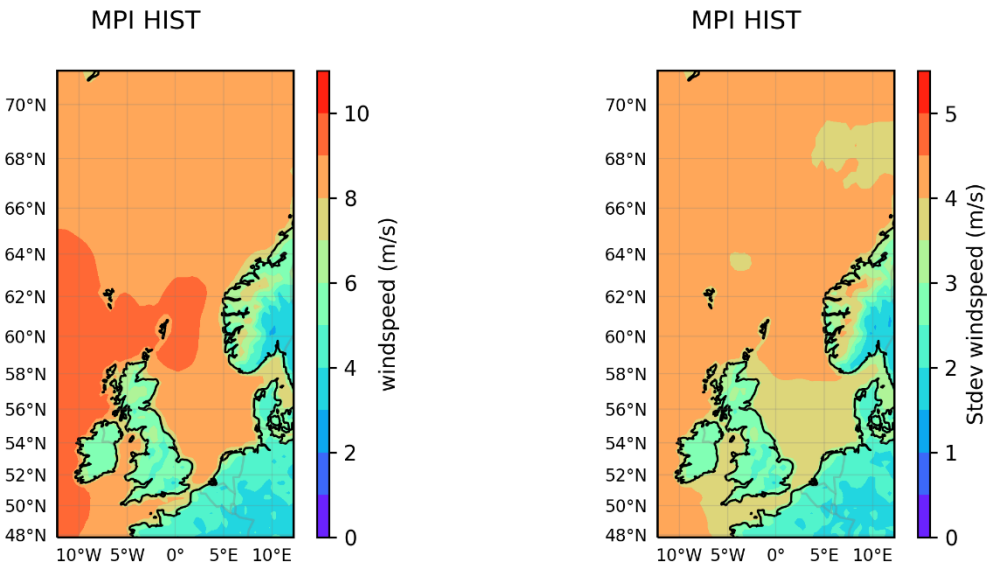

Figure 60: Mean wind speed map and standard deviation for MPI

12.3. RCP8.5 runs

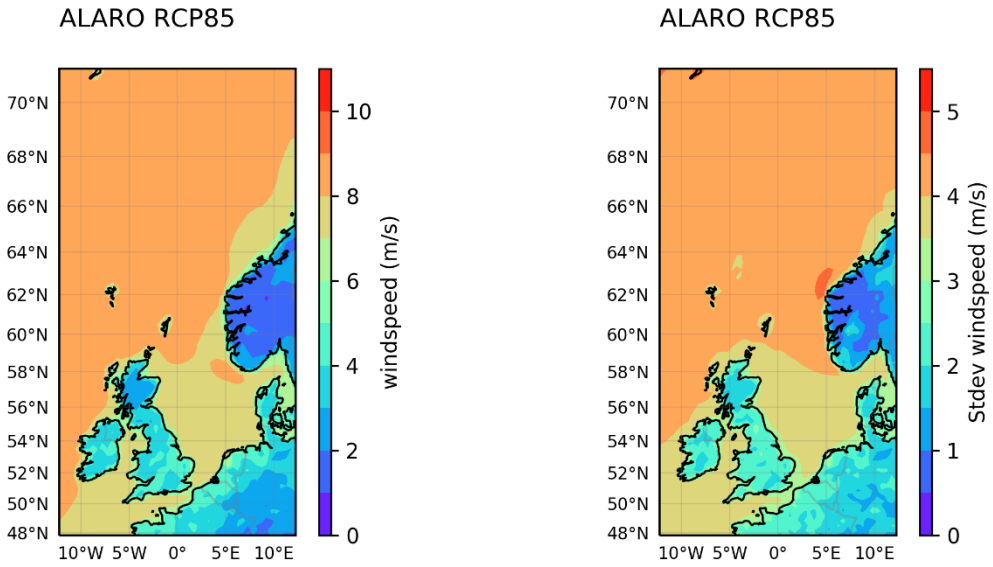

Figure 61: Mean wind speed map and standard deviation for ALARO

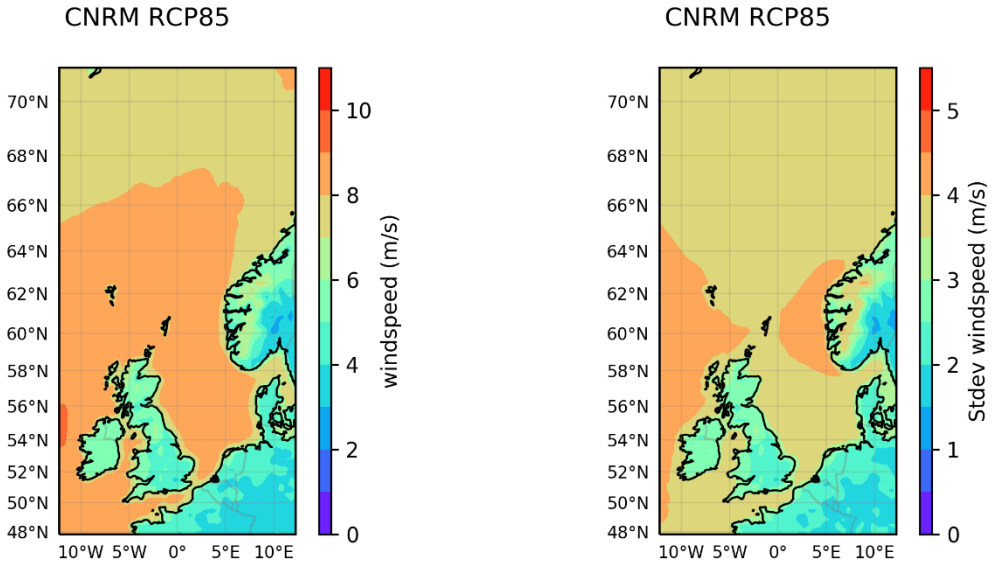

Figure 62: Mean wind speed map and standard deviation for CNRM

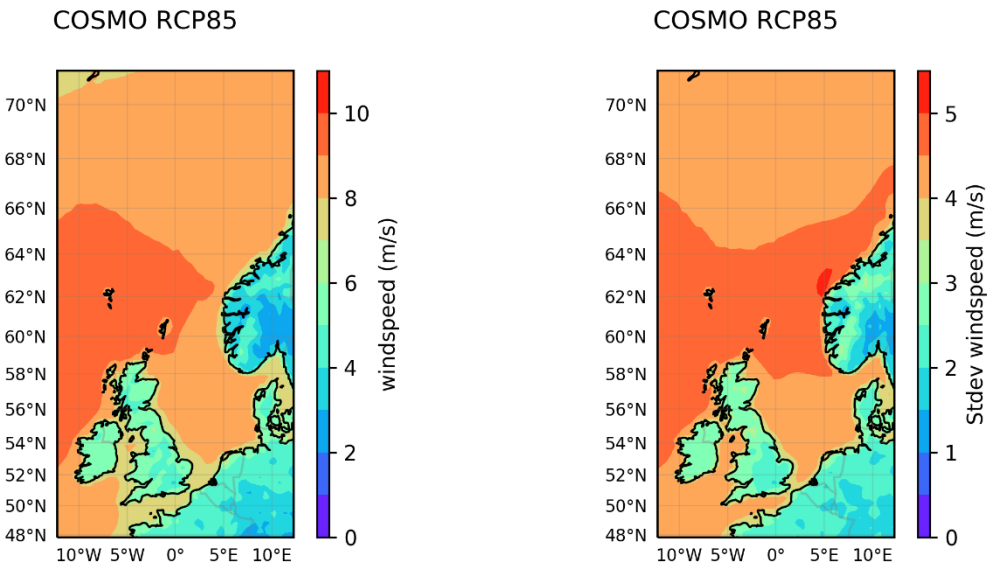

Figure 63: Mean wind speed map and standard deviation for COSMO

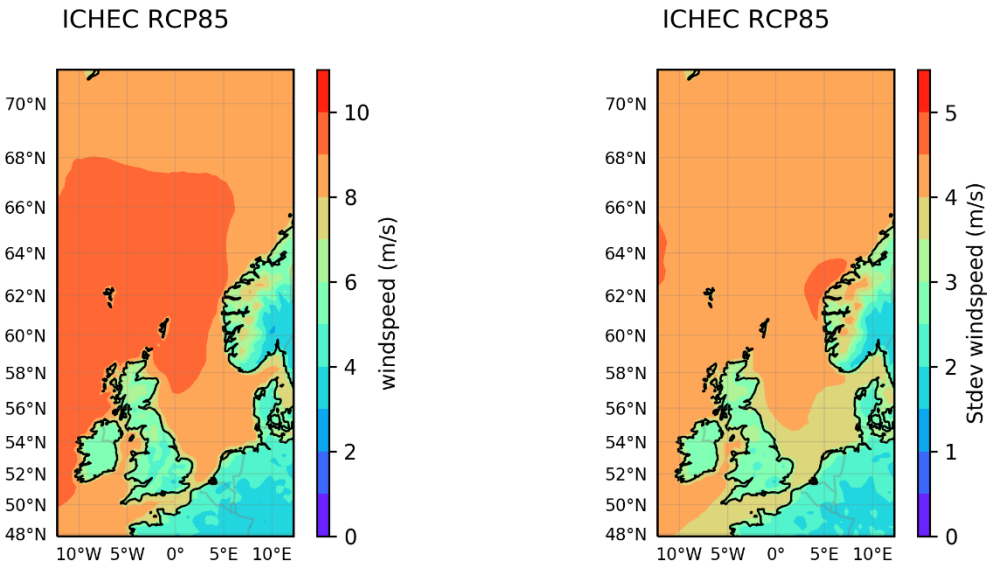

Figure 64: Mean wind speed map and standard deviation for ICHEC

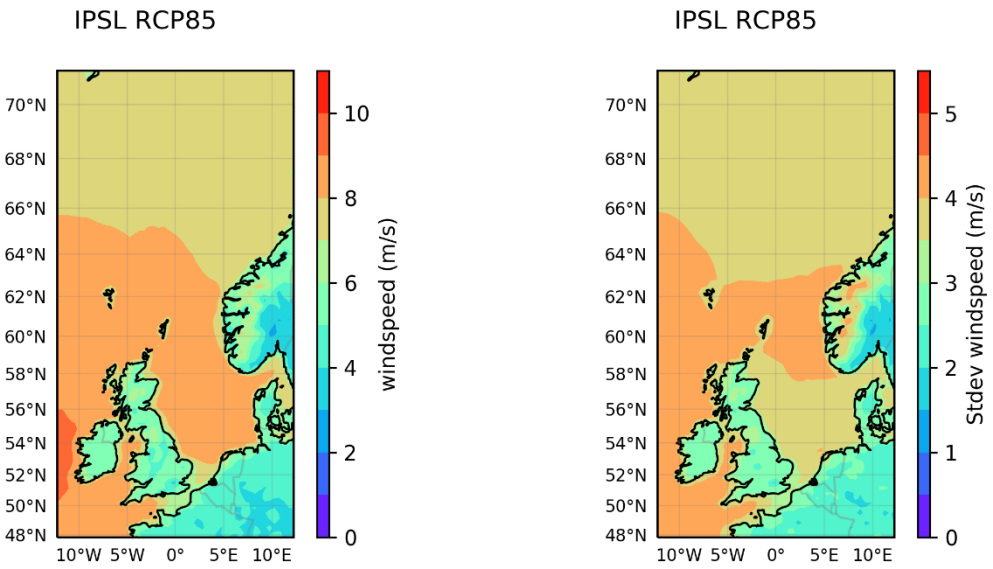

Figure 65: Mean wind speed map and standard deviation for IPSL

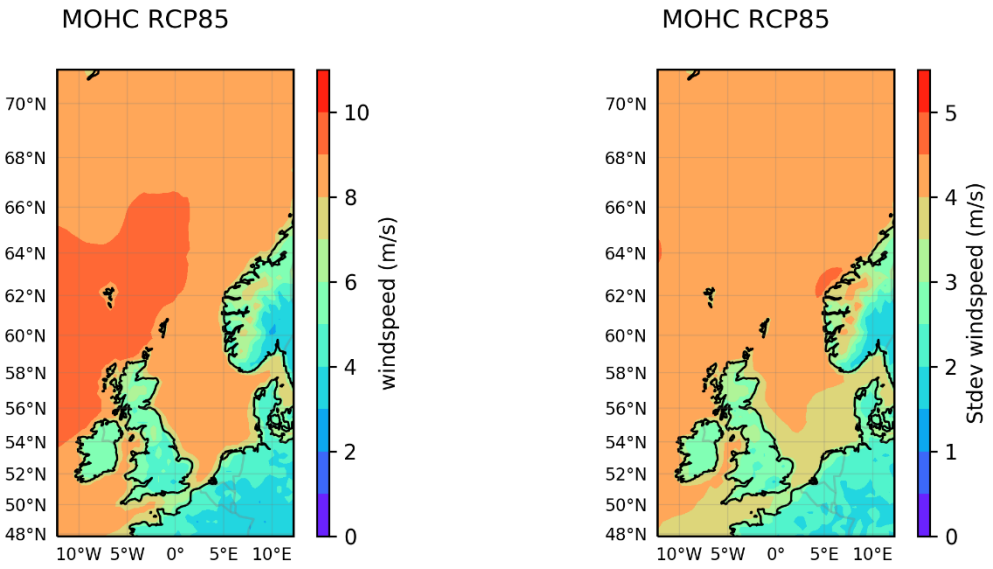

Figure 66: Mean wind speed map and standard deviation for MOHC

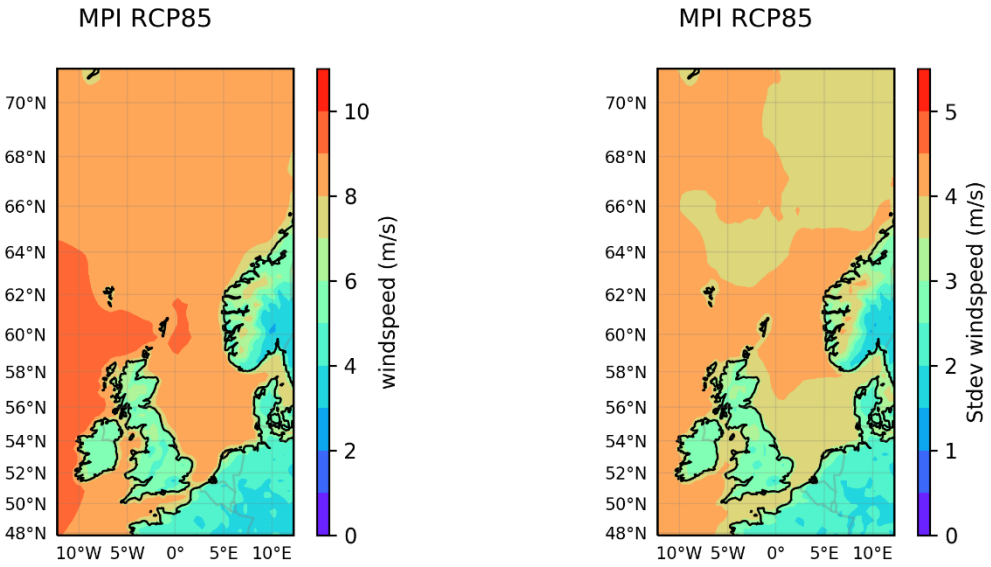

Figure 67: Mean wind speed map and standard deviation for MPI

COLOPHON

This report was issued by Operational Directorate Natural Environment in March 2019.

The reference code is CREST/X/DVDE/201903/EN/TR01.

Status ☒ draft
☐ final version
☐ revised version of document
☐ confidential

Available in ☒ English
☐ Dutch
☐ French

If you have any questions or wish to receive additional copies of this document, please send an e-mail to *DVandenEynde@naturalsciences.be*, quoting the reference, or write to:

Royal Belgian Institute of Natural Sciences
Operational Directorate Natural Environment
100 Gulledelle
B–1200 Brussels
Belgium
Phone: +32 2 773 2111
Fax: +32 2 770 6972
http://www.mumm.ac.be/

Royal Belgian Institute of Natural Sciences
Operational Directorate Natural Environment
Suspended Matter and Seabed Monitoring and Modelling Group

The typefaces used in this document are Gudrun Zapf-von Hesse's *Carmina Medium* at 10/14 for body text, and Frederic Goudy's *Goudy Sans Medium* for headings and captions.